

Software Interface Specification for the Venus Climate Orbiter Akatsuki Radio Science Data Products

Version 1.3

July 16, 2025

Prepared by

Armin Kleinböhl¹, Shin-ya Murakami², Takeshi Imamura³, Shigeru Suzuki¹, Hiroki Ando⁴

- 1 Jet Propulsion Laboratory, California Institute of Technology
- 2 Japan Aerospace Exploration Agency
- 3 The University of Tokyo
- 4 Kyoto Sangyo University



Table of Contents

| | |
|---|----|
| Change Log..... | iv |
| Acronyms and Abbreviations | v |
| 1 Purpose and Scope of Document..... | 1 |
| 2 Applicable Documents | 1 |
| 3 Data Product Characteristics and Environment | 1 |
| 3.1 Measurement Overview..... | 1 |
| 3.2 Data generation and downlink..... | 4 |
| 3.3 Data Product Overview | 5 |
| 3.4 Data Processing | 5 |
| 3.4.1 Data Processing Levels..... | 5 |
| 3.4.2 Data Product Generation..... | 6 |
| 3.4.3 Data Flow..... | 10 |
| 3.4.4 Labeling and Identification | 10 |
| 3.5 Standards Used in Generating Data Products..... | 12 |
| 3.5.1 PDS Standards..... | 12 |
| 3.5.2 Time Standards | 12 |
| 3.5.3 Coordinate Systems | 12 |
| 3.5.4 Data Storage Conventions | 13 |
| 3.6 Data Validation..... | 13 |
| 3.7 Data Quality and Coverage..... | 13 |
| 4 Detailed Data Product Specifications | 23 |
| 4.1 Data Product Structure and Organization | 23 |
| 4.2 Data Format Descriptions..... | 24 |
| 4.2.1 Level 1 - Raw Data | 24 |
| 4.2.2 Level 2 – Calibrated Data..... | 30 |
| 4.2.3 Level 3 – Derived Data | 32 |
| 4.2.4 Level 4 - Derived Data..... | 33 |
| 5 Applicable Software | 35 |
| 5.1 Utility Programs..... | 35 |
| 5.2 Applicable PDS Software Tools..... | 35 |
| 5.3 Software Distribution and Update Procedures | 35 |
| 6 Appendices..... | 36 |
| 6.1 References..... | 36 |

| | | |
|-----|--|----|
| 6.2 | Definitions of Data Processing Levels..... | 36 |
|-----|--|----|

Change Log

| DATE | CHANGE | AFFECTED SECTIONS |
|------------|---|---------------------|
| 2016-07-06 | Initial Draft | All |
| 2023-04-26 | Second Draft | All |
| 2023-07-31 | Version 1.0 | All |
| 2024-03-01 | Version 1.1 Added description on zero paddings to RS Level 1 data. | 3.4.2.1 |
| 2024-06-13 | Version 1.2 Added mission logo. Changed extension of the PDS4 label. | Front page 3.4.4 |
| 2025-07-16 | Version 1.3 Added descriptions for the observations during 2023 and 2024. Added extension for the PDS3 label. | 3.7 3.4.4 |
| | | |
| | | |

Acronyms and Abbreviations

| Acronym/Abbreviation | Definition |
|----------------------|---|
| A/D | Analog to Digital |
| ATM | PDS Atmospheres node |
| ASCII | American Standard Code for Information Interchange |
| CCSDS | Consultative Committee for Space Data System |
| DARTS | Data ARchives and Transmission System |
| Delta-DOR | Delta-Differential One-way Ranging |
| DLR | German Aerospace Center (Deutsches Zentrum für Luft- und Raumfahrt) |
| DSV | Delimiter Separated Values |
| HGA | High-gain antenna |
| IAU | International Astronomical Union |
| ID | Identifier |
| IDSN | Indian Deep Space Network |
| IPDA | International Planetary Data Alliance |
| ISAS | Institute of Space and Astronautical Science |
| JAXA | Japan Aerospace Exploration Agency |
| LSK | Leapseconds kernel |
| N/A | Not Available |
| NICT | National Institute of Information and Communications Technology |
| PDS | Planetary Data System |
| RDEF | Raw Data Exchange Format |
| RS | Radio Science |
| SCLK | Spacecraft Clock Kernel |
| SIRIUS | Scientific Information Retrieval and Integrated Utilization System |
| SIS | Software Interface Specification |
| S/N | Signal to noise (ratio) |
| SPICE | Spacecraft, Planet, Instrument, C-Matrix, Events |
| SPIDAr | SPICE and Data Archive (team) |
| SPK | Ephemeris data kernel |
| UDSC | Usuda Deep Space Center |
| USO | Ultra-stable Oscillator |
| UTC | Coordinated Universal Time |
| VCO | Venus Climate Orbiter |
| VIRA | Venus International Reference Atmosphere |
| VSSP | Versatile Scientific Sampling Processor |
| WHM | Wheilheim (station of DLR) |
| XHGA | X-band High-gain Antenna |
| XMGA | X-band Medium-gain Antenna |
| XML | Extensible Markup Language |

1 Purpose and Scope of Document

The purpose of this Data Product Software Interface Specification (SIS) is to provide users of the data products from the Radio Science (RS) with a detailed description of the products derived from radio occultations in Akatsuki mission and how each product was generated, including data sources and destinations.

The purpose of this Data Product Software Interface Specification (SIS) is to provide users of the raw, calibrated, and derived data products from the Venus Climate Orbiter (VCO) Akatsuki Radio Science experiments (RS) with a detailed description of the products, and a description of the product generation procedures, including data sources and destinations. The products defined in this document are raw, calibrated, and derived data.

This SIS is intended to provide enough information to enable users to read and understand the data products as stored in the Data ARchives and Transmission System (DARTS) and the Planetary Data System (PDS). The users for whom this document is intended are the scientists who will analyze the data, including those associated with the project and those in general planetary science community.

2 Applicable Documents

This SIS is consistent with the following Planetary Data System Documents as adopted by the International Planetary Data Alliance (IPDA):

1. Planetary Data System Standards Reference, Version 1.19.0, <https://doi.org/10.17189/02p7-vj89>, October 1, 2022.
2. PDS4 Data Dictionary – Abridged – Version 1.19.0.0, September 19, 2022.
3. PDS4 Information Model, Version 1.19.0.0, September 19, 2022.

This SIS references the following documents:

4. Imamura, T., et al., RS: Radio Science investigation of the Venus atmosphere and ionosphere with Venus orbiter, Akatsuki, *Earth, Planets and Space*, **63**, 493–501. <https://doi.org/10.5047/eps.2011.03.009>, 2011.
5. Imamura, T., et al., Initial performance of the radio occultation experiment in the Venus orbiter mission Akatsuki, *Earth, Planets and Space*, **69**, 137, <https://doi.org/10.1186/s40623-017-0722-3>, 2017.
6. Kondo, T., K5/VSSP and K5/VSSP32 Data Format, Technical Development Center Technical Report, National Institute of Information and Communications Technology, 2010. https://www2.nict.go.jp/sts/stmg/K5/VSSP/vssp_format-e.100820.pdf
7. CCSDS – The Consultative Committee for Space Data Systems, Recommended Standard for Delta-DOR Raw Data Exchange Format, CCSDS 506.1-B-1, 2013, <https://public.ccsds.org/Pubs/506x1b1.pdf>.

A complete list of the references is found at [Appendix 6.1](#).

3 Data Product Characteristics and Environment

3.1 Measurement Overview

The following descriptions are partially extracted from [Imamura et al. \(2011, 2017\)](#).

The primary goal of Akatsuki RS is to characterize the meteorological processes that might drive the planet-wide easterly wind (super-rotation) as well as to understand the cloud dynamics. For this

purpose, the temporal and spatial variability of the Venus atmosphere will be studied by retrieving the vertical profiles of the temperature, the H_2SO_4 vapor density, and the intensity of small-scale density fluctuations. Another goal of Akatsuki RS is to study the spatial and temporal variabilities of the ionosphere in response to variations in the solar wind and the neutral atmosphere by measuring ionospheric electron density profiles. Finally, the investigation of the properties of the solar wind plasma is also an objective of Akatsuki RS.

The schematic of a radio occultation measurement is shown in Figure 1. Radio waves are transmitted from the spacecraft, refracted in the planetary atmosphere, and received at a ground station. For a radially symmetric atmosphere the asymptotic bending angle α is related to the refractive index n as (e.g., Fjeldbo et al., 1971):

$$\alpha(a) = -2a \int_{r_0}^{\infty} \frac{1}{n} \frac{\partial n}{\partial r} \frac{dr}{\sqrt{(nr)^2 - a^2}}, \quad (1)$$

where a is the ray impact parameter, r is the radius, and r_0 is the radius of the closest approach given by Bouguer's rule:

$$n(r_0)r_0 = a. \quad (2)$$

The asymptotic bending angle α and the ray impact parameter a are calculated from the measured atmospheric Doppler shift and the reconstructed velocity and position vectors of the spacecraft and the ground station. For a radially symmetric atmosphere, the refractive index n is obtained as a function of the radius r from the relationship between α and a through Abel transformation:

$$\ln n(r) = -\frac{1}{\pi} \int_{a_1}^{\infty} \ln \left\{ \frac{a}{a_1} + \left[\left(\frac{a}{a_1} \right)^2 - 1 \right]^{\frac{1}{2}} \right\} \frac{d\alpha}{da} da, \quad (3)$$

where a_1 is the impact parameter for a ray whose radius of closest approach is r , and a_1 and r are related with each other through Bouguer's rule. The deviation of the refractive index n from unity is the sum of the contributions from the neutral atmosphere and the ionosphere:

$$n - 1 = VN \times 10^{-6} - \frac{\beta N_e}{f^2}, \quad (4)$$

where V is the refractive volume, N is the number density of the neutral atmosphere, $\beta = e^2/8\pi^2\epsilon_0 m_e \sim 40.3 \text{ m}^3\text{s}^{-2}$ with e , ϵ_0 , m_e being the elementary charge, the dielectric constant in vacuum, and the electron mass, respectively, N_e is the number density of electrons, and f is the frequency of the carrier signal. On the assumption that the neutral atmosphere is well mixed, we adopt a constant V of $1.811 \times 10^{-23} \text{ m}^3$ that is appropriate for the composition of 96.5% CO_2 and 3.5% N_2 following Tellmann et al. (2009). The neutral and ionospheric contributions are almost separated in altitude with the boundary around 100 km altitude; this enables us to retrieve the vertical profiles of the neutral atmospheric density N and the electron density N_e separately.

The vertical profile of the neutral atmospheric pressure, $p(r)$, is derived from the density profile $N(r)$ by integrating the equation of hydrostatic equilibrium:

$$p(r) = p(r_{\text{top}}) + m \int_r^{r_{\text{top}}} N(r') g(r') dr', \quad (5)$$

where m is the mean molecular mass that is taken to be 43.44 u (Seiff et al. 1985), $g(r)$ is the altitude-dependent acceleration due to gravity, and r_{top} is the upper boundary, which is taken to be around 90–100 km altitude. The product of the gravitational constant and the mass of Venus used for calculating $g(r)$ is $GM = 3.24858592 \times 10^{14} \text{ m}^3\text{s}^{-2}$ following the value adopted in the SPICE PCK, gm_de431.tpc, provided by NAIF. The ideal gas law relates $p(r_{\text{top}})$ to the atmospheric temperature at this height, $T(r_{\text{top}})$, as $p(r_{\text{top}}) = N(r_{\text{top}})kT(r_{\text{top}})$, where k is the Boltzmann's constant. The boundary

condition $T(r_{\text{top}})$ is determined empirically. The temperature profile $T(r)$ is calculated from $N(r)$ and $p(r)$ using the ideal gas law. The influence of $T(r_{\text{top}})$ on $T(r)$ becomes negligibly small around 10 km below r_{top} (Tellmann et al. 2009).

The height range of the Venus' neutral atmosphere accessible by radio occultation is approximately 32-90 km. Below 40 km the defocusing loss and the attenuation by the atmosphere limits the quality of the observation, and 32 km is the lowest accessible altitude, below which the radius of curvature of the ray path becomes smaller than the distance to the planet's center.

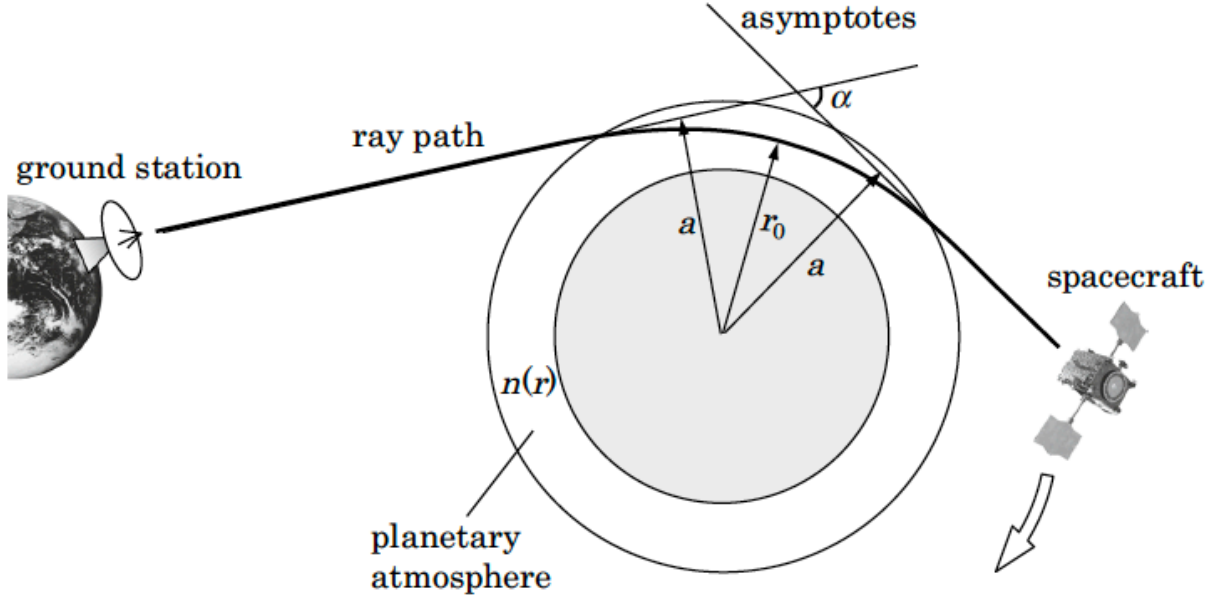


Figure 1: Schematic of a radio occultation experiment. This figure was taken from Figure 1 in Imamura et al. (2017).

The vertical resolution d is limited by the diameter of the first Fresnel zone, which is given by (Häusler et al. 2006; Imamura et al. 2011)

$$d = 2\sqrt{\lambda DL}, \quad (6)$$

where λ is the wavelength of the carrier signal, D is the distance from the spacecraft to the crossing of the ray asymptotes, and L is the defocusing loss. Above ~ 90 km altitude, where defocusing loss is negligible ($L = 1$), d ranges from 1.0 to 1.8 km in Akatsuki radio occultation experiments conducted by April 2017 because of the change of D in the range 7000–23,000 km. Although the distance between Akatsuki and Venus changes significantly along the orbit, radio occultation mostly occurs when the spacecraft is located near periapsis. The d becomes smaller at lower altitudes because of the smaller L : it is 0.4–0.5 km at 75 km altitude in the same period.

RS relies on the extreme frequency stability of both the onboard radio wave source and the recording system at the ground station. Akatsuki RS employs an ultra-stable oscillator (USO) as an onboard reference frequency source (Figure 2). The USO provides a stable reference frequency (38.22567759 MHz) for the transponder. It was manufactured by TimeTech GmbH in Germany and is a heritage from the USOs flown onboard the ESA's Rosetta and Venus Express spacecraft. We made several modifications such as the redesign of the thermal insulation and mechanical shock protection system to adapt to the higher mechanical loads during the launch, resulting in dimensions (17 cm \times 13 cm \times 16 cm) and mass (1.9 kg) that are greater than for previous USOs. The USO is characterized by

excellent frequency stability; the Allan deviation is on the order of 10^{-13} at the integration time from 1 to 1000 s.



Figure 2: Photograph of the USO onboard Akatsuki.

The USO was switched on in June 2010, just after the launch, but was switched off from July 2011 to December 2015. To evaluate the stability of the USO output frequency after the launch, downlink signals generated by the USO were recorded several times at UDSC before July 2011 and during the initial checkout phase after December 2015. An analysis of the data showed that the long-term drift of the output frequency was found to be less than $\sim 3 \times 10^{-8}$ times the nominal frequency. The derived frequency stability was $< 10^{-12}$ for the averaging time of 1–1000 s, and no notable degradation was observed after the launch. This stability corresponds to a frequency resolution of ~ 0.01 Hz, which assures discrimination of atmospheric temperature fluctuations with a magnitude of 0.1 K imposed on adjacent two layers separated by 1 km (Imamura et al. 2011).

3.2 Data generation and downlink

Observations are conducted only when the spacecraft is hidden by Venus as seen from the ground station. Recording of the signal at the ground station starts ~ 15 minutes before the start of the occultation and ends ~ 15 minutes after the end of the occultation. One-way downlink at X-band (8410.932 MHz), stabilized by the onboard ultra-stable oscillator, is used in the experiments. During the experiments, one of the X-band transponders (XTRP) is locked to the USO, and the transponder signal is amplified by the 23.4 W traveling wave tube amplifier (TWTA). The gain of the 0.9 m-diameter flat-type slot array antenna (XHGA-T) is 35 dBi, corresponding to a 3 dB full beam width of $\sim 2^\circ$. Since the ray bending far exceeds the beam width, the spacecraft performs attitude maneuvers to compensate for the changing direction of the signal path. The equivalent isotropically radiated power (EIRP) is 42.5 dBW when the TWTA is used. The radio wave transmitted by the spacecraft is received at the Usuda Deep Space Center (UDSC) in Japan. The 64-m dish provides a gain of 72.5 dBi including the feeder loss in X-band, at a system noise temperature of 96 K for a 5 mm hour $^{-1}$ rain and an elevation angle of 15° . The received signals are down-converted by an open-loop heterodyne system stabilized by a hydrogen maser (Allan deviation $< 3 \times 10^{-13}$ for 1 s, $< 3 \times 10^{-15}$ for 1000 s) and digitized.

In addition to UDSC, two other ground stations have been used to receive Akatsuki RS signals. A summary of the key parameters of the ground stations is given in Table 1. The receiving ground station is reflected in the file name of each data file with its abbreviated station name followed by the antenna diameter in meters. Usuda Deep Space Center (UDSC64) and Indian Deep Space Network (IDSN32)

provide open-loop recording, while Weilheim Ground Station (WHM30) provides closed-loop recording.

Table 1: Key parameters of ground stations used to receive Akatsuki RS signals.

| Station | Operating agency | Location | Coordinates | Antenna diameter | Abbreviation |
|---------------------------|--|--|-------------------------|------------------|--------------|
| Usuda Deep Space Center | Japanese Aerospace Exploration Agency (JAXA) | Saku, Nagano prefecture, Japan | 36°07'44"N, 138°21'54"E | 64 m | UDSC64 |
| Indian Deep Space Network | Indian Space Research Organisation (ISRO) | Byalalu, Ramanagar district, Karnataka, India | 12°54'11"N, 77°22'08"E | 32 m | IDSN32 |
| Weilheim Ground Station | German Aerospace Center (DLR) | Weilheim, Weilheim-Schongau district, Bavaria, Germany | 47°52'52"N, 11°04'42"E | 30 m | WHM30 |

Some observations were performed with one of the X-band medium gain antennas (XMGA) because of spacecraft attitude limitations, although the 17 dB lower gain of XMGA relative to XHGA-T degrades the measurements. If the XMGA was used, it was noted to the XML label of the data file.

3.3 Data Product Overview

Radio science data products consist of raw data received at the station, calibrated data providing Doppler and signal amplitudes, and derived data that includes bending angles and impact parameters as well as profiles of atmospheric parameters vs. cytherocentric tangent radius. All data files except for raw data products are provided in ASCII format. For atmospheric profile data a browse product is also provided in PDF format. Descriptions of data fields and metadata are provided in PDS4-compliant XML labels. The RS data products are:

1. **RS Raw Data Product:** Raw open-loop signal measurements of Akatsuki X-band radio occultation observations collected by open-loop receiving equipment at the 64-m Usuda Deep Space Center (UDSC) antenna and other stations.
2. **RS Calibrated Data Product:** Doppler and signal amplitude measurements derived from the Raw Data Product.
3. **RS Derived Data Product:** Refractivity, bending angle as a function of impact parameters including cytherolocation derived from Akatsuki radio occultation data. Atmospheric density, pressure and temperature profiles as a function of cytherocentric radius including cytherolocation derived from the Calibrated Data Product.
4. **RS Browse Data Product:** Quick look data product providing cytherolocation of profile data on a map and graphs of density, pressure and temperature profiles vs. altitude.

3.4 Data Processing

This section of the SIS provides general information about data product content, format, size, and production rate. The specifics of the data product formats are discussed in [Section 4](#).

3.4.1 Data Processing Levels

Due to the different nature of the RS experiment in comparison to the camera investigations, the definitions of the processing levels for RS differ from the processing levels for the UVI, IR1, IR2, and LIR instruments ([Ogohara et al. 2017](#)). [Table 2](#) provides processing level of each product in both

Akatsuki project terms and PDS4 terms, the processing level the data originated from, and a brief description of the data at each processing level. All data products are provided on the DARTS as well as on the PDS.

Table 2: List of RS data processing level.

| Processing Level | PDS4 Processing Level | Description | Processing level from which data is derived |
|------------------|-----------------------|---|---|
| Level 1 | Raw | Raw open-loop data composed of voltage time series of the downlink signal received at the ground station. | - |
| Level 2 | Calibrated | Time series of the Doppler frequency and the signal level. | Level 1 |
| Level 3 | Derived | Time series of the bending angle, the impact parameter, the closest approach of the bended ray to the planet, and the atmospheric refractivity at the closest approach. | Level 2 |
| Level 4 | Derived | Profiles of atmospheric number density, pressure, and temperature vs. cytherocentric tangent radius. | Level 3 |
| Browse | Derived | Browse product providing cytherolocation of profile data on a map and graphs of density, pressure and temperature profiles vs. altitude. | Level 4 |

3.4.2 Data Product Generation

All data products and associated documentation are generated by the RS team and the SPIDAr team. The PDS ATM assists in the definition and development of first delivery products and their associated PDS documentation, which will act as templates for subsequent updates. When new products are developed by the RS team, PDS ATM will likewise assist in the definition and development of those products and their associated PDS documentation in preparation for their initial delivery.

3.4.2.1 Level 1

RS Level 1 data are raw open-loop signal measurements of Akatsuki X-band radio occultation observation as received by the ground station. Raw data from the UDSC and IDSN (Indian Deep Space Network) stations are open-loop recordings, with files from the UDSC station provided in K5/VSSP format or K5/VSSP32 format ([Kondo 2010](#)) and files from the IDSN station provided in CCSDS Delta-DOR Raw Data Exchange Format (RDEF) Product File ([CCSDS 2013](#)). Files for solar corona observation from UDSC after 2016 were provided in CCSDS Delta-DOR RDEF Product File. Data are in binary format and comes with PDS4-compliant detached XML labels. No Level 1 data from the WHM30 station are included because the closed-loop recorder directly yielded observed frequency data, which are identical to those in the Level 2 data in this bundle.

The radio wave at X-band (8.410926 GHz) transmitted by the spacecraft is received at the ground station. The received signal is heterodyned to a synthetic signal (baseband) stabilized by a hydrogen maser based on the predicted Doppler-shifted downlink frequency to obtain a narrow-band signal with a center frequency of several hundred kHz (downconversion), and then digitized. The frequency of the baseband used for down-conversion is constant in each experiment and available as `vco:RS_Experiment_Attributes / vco:downconversion_frequency` in Hz, in the associated XML label.

The sampling rate is 1 MHz or more so that the carrier signal can be confined in the recording bandwidth. The raw data is defined as Level 1.

The transmitted signal is right-handed circularly polarized (RHCP) and only the RHCP signal is recorded on the ground for Venus atmosphere observations. In the solar corona observations after 2016, right- and left-handed circularly polarized (LHCP) signals were recorded to files separately. One can identify which signal was recorded, LHCP or RHCP, by filename or `vco:RS_Experiment_Attributes / vco:circular_polarization` in the XML label.

The last record of the RS Level 1 data may have incomplete data, so zeros were appended as padding. How many bytes of zeros were appended can be found at `vco:RS_Experiment_Attributes / vco:last_zero_padding_size` in the XML label.

3.4.2.2 Level 2

In the processing of recorded data, first the Doppler shift calculated from the orbital information and a model of the Venus atmosphere is subtracted from the original signal by heterodyning, thereby suppressing the frequency variation and enabling narrow-band filtering. Then, approximate carrier frequencies are determined for successive time blocks by fitting a theoretical signal spectrum (sinc function) to the discrete Fourier transforms. The resultant frequency variation is subtracted from the signal by heterodyning in order to apply another narrow-band filtering.

The filtering scheme automatically converts the data to a complex representation, in which each datum comprises both the amplitude and phase of the signal. The low-noise signal generated by narrow-band filtering yields the phase by removing cycle slips via the phase unwrapping procedure. The frequency is obtained by differentiating the phase with respect to time. The sum of the frequency variation in this final product and the frequency variations that have been subtracted via heterodyning in the course of the processing gives the total atmospheric Doppler frequency. The Level 2 data contains the derived Doppler frequency and the signal level, which is also obtained in the course of the analysis above.

Data is reported as “Observed X-Band Antenna Frequency”, which is the frequency of the signal at the receiving antenna at UTC Time, and “Predicted X-Band Antenna Frequency”, which is the expected frequency of the signal at the receiving antenna at "UTC Time" based on the VCO Akatsuki reconstructed SPKs. The calculation includes geometrical effects (relative positions and motions of ground station and spacecraft, including the Earth rotation and light time adjustments). Correction for propagation through the Earth's neutral atmosphere is not made. The difference between these two frequencies, reported as “Residual Calibrated X-Band Frequency Shift” corresponds to the atmospheric Doppler shift from which atmospheric profiles are obtained in subsequent data levels. Note that raw data from the WHM30 station are identical to “Observed X-Band Antenna Frequency” and “Residual Calibrated X-Band Frequency Shift”.

The 3 dB half beam width of the high-gain antenna is $\sim 1^\circ$. Since the ray bending in the Venus atmosphere exceeds the beam width of high-gain antenna (HGA), the spacecraft performs attitude maneuvers to compensate for the changing direction of the signal path. The direction of the antenna beam is changed along a polygonal (zigzag) curve in such a way that the difference between the controlled beam direction and the ideal beam direction based on the Venus International Reference Atmosphere (VIRA) (Seiff et al. 1985) is less than 0.05° . The difference sometimes exceeds this limit because of an inaccurate trajectory prediction at the time of command generation or no attitude maneuver due to limitation of spacecraft operation, leading to non-negligible decline of the signal intensity. The effect of such antenna mispointing on the measured intensity is corrected using the measured antenna pattern (Toda et al. 2010) and the trajectory data reconstructed after the experiment. The parameters used for correcting the signal intensity due to antenna mispointing are given in Table

3. The accuracy of this intensity correction is estimated to be better than 1 dB in most of the cases. Before the intensity correction, the noise level was estimated from the portion of the data dominated by noise and then the estimated noise component was subtracted from the whole time series.

Table 3: Antenna pattern used for correcting signal intensity due to antenna mispointing.

| Offset angle from boresight (deg) | HGA gain (dB) |
|-----------------------------------|---------------|
| 0 | 35.6 |
| 0.5 | 35.135 |
| 1 | 33.7 |
| 1.5 | 31.135 |
| 2 | 27.055 |
| 2.5 | 20.495 |
| 3 | 9.075 |
| 3.5 | 14.815 |
| 4 | 16.34 |
| 4.5 | 13.89 |
| 5 | 6.44 |

3.4.2.3 Level 3

Atmospheric profiles are obtained from the frequency variation caused by the Venus atmosphere observed at the tracking station. Subtraction of the total Doppler shift from the “straight-line Doppler shift”, which is the frequency variation that were observed if Venus did not exit, gives the contribution of the Venusian atmosphere termed “atmospheric Doppler shift”. This frequency component is given in the RS Level 2 data as “residual calibrated X-band frequency shift”. Although the atmospheric Doppler shift should be zero in the portion of the data above the height of the ionosphere, we usually observe a smoothly-varying frequency component that is attributed to the error in the trajectory data. To remove this frequency offset, we fit a linear function to this portion of the frequency time series and subtract it from the whole time series; this procedure is termed “baseline fit”. The atmospheric Doppler shift corrected by baseline fit is combined with the trajectory data to calculate the bending angle as a function of the impact parameter, which are given in RS Level 3 data.

The relationship between the bending angle and the impact parameter is converted to a refractive index profile through Abel transform (eq. (3)). For the integration with respect to the impact parameter in Abel transformation, the bending angle needs to be a single-valued function of the impact parameter. However, the bending angle sometimes becomes a multivalued function of the impact parameter at low altitudes due to low signal-to-noise ratios. To suppress such multivalued behavior, the integration time is increased in those regions, and extreme outliers are removed by visual inspection.

RS Level 3 data is provided in separate files for ingress geometry (marked with an “i” in the file name) and for egress geometry (marked with an “e” in the file name). Note that not all occultation observations will have both ingress and egress data.

3.4.2.4 Level 4

The deviation of the refractive index from unity is the sum of the contributions from the neutral atmosphere and the ionosphere. The neutral and ionospheric contributions are separated in altitude with the boundary around 100 km altitude; this enables us to retrieve the vertical profiles of the neutral atmospheric density and the electron density separately. Number density profiles of the atmosphere are obtained from refractive index using [eq. \(4\)](#). Vertical profiles of the neutral atmospheric pressure are derived from the density profiles by integrating the equation of hydrostatic equilibrium ([eq. \(5\)](#)). Temperature profiles are calculated from the density and the pressure profiles using the ideal gas law. Values for a refractive volume, mean molecular mass, and planetary mass times gravitational constant used for this analysis are given in [Section 3.1](#). This results in vertical profiles of atmospheric number density, temperature and pressure as a function of cytherocentric tangent radius that constitute RS Level 4 data. The upper boundary of the pressure and temperature profiles are set at 95 km. The boundary condition for the temperature, which is needed for integration, is set empirically to a value of 170 K (“medium temperature at boundary”). In order to illustrate the influence of this boundary condition on the retrieved profile, alternative profiles in which this boundary condition is set to 140 K (“lower temperature at boundary”) and 200 K (“higher temperature at boundary”), respectively. Alternative profiles of pressure that correspond to these respective boundary conditions are reported accordingly. No electron density or sulfuric acid mixing ratio data are provided in the current release of Level 4 data. These quantities will be provided in a future release.

Similar to RS Level 3 data, RS Level 4 data is provided in separate files for ingress geometry (marked with “ai” in the file name) and for egress geometry (marked with “ae” in the file name). Note that not all occultation observations will have both ingress and egress data. Profiles derived from ingress data are reported with decreasing tangent radius such that the top entry of the file corresponds to the highest altitude in the profile. Profiles derived from egress data are reported with increasing tangent radius such that the top entry of the file corresponds to the lowest altitude in the profile.

3.4.2.5 Browse – Browse data

In order to make it easier for the user to gain an overview over Akatsuki Radio Science a quick-look data product for visualizing RS Level 4 data has been created. It consists of files in PDF format, together with PDS4-compliant detached XML labels. Each PDF file corresponds to one RS Level 4 profile retrieval. Each PDF file has four panels:

- Top left panel: Tangent point locations color-coded by tangent altitude overlaid over a topographic map derived from Magellan data.
- Bottom left panel: Profile of atmospheric number density.
- Bottom right panel: Profiles of atmospheric pressure, color coded for different boundary temperatures at the top of the atmosphere.
- Top right panel: Profiles of atmospheric temperature, color coded for different boundary temperatures at the top of the atmosphere.

A topographic map derived from Magellan data is used to create the image in the top left panel. The topographic map is the version 2 (1997 release) of the Global Topographic Data Record (GTDR-SINUS.3;2) from [Ford \(1992\)](#).

Numbers in bottom left panel, bottom right panel and top right panel indicate the sample number of the first and last data point of the profile given in the corresponding RS Level 4 data file. Profiles are given with as a function of geometric altitude. Geometric altitude is calculated by subtracting the Venus spherical radius, fixed at a value of 6051.8 km, from the cytherocentric tangent radius provided in the corresponding RS Level 4 data file. Equivalent to the RS Level 4 data it is derived from, browse

data is provided in separate files for ingress geometry (marked with “ai” in the file name) and for egress geometry (marked with “ae” in the file name).

3.4.3 Data Flow

Level 1 data acquired at the UDSC antenna and the IDSN antenna were transferred via sftp to a workstation of the RS team. Level 1 K5/VSSP and K5/VSSP32 data acquired at the UDSC antenna was reformatted by concatenating all separate data files for each observation, and adding zero-padding to the end of the file. Level 1 CCSDS Delta-DOR RDEF data acquired at the UDSC and IDSN antennas were just renamed to follow the Akatsuki RS L1 data filename convention. Level 2 data acquired at the Weilheim antenna of DLR were sent via email to the RS team. All higher-level data products were created by the RS team using their computers, and then they were delivered to the Reformatter at ISAS/JAXA.

3.4.4 Labeling and Identification

All RS data products are labeled with PDS4 compliant detached XML labels. These labels describe the content and format of the associated data product. Labels and products are associated by file name with the label having the same name as the data product except that the label file has a .lblx extension.

Labels are constructed with the PDS4 Product Class, Product_Observational sub-class. The Product_Observational sub-class describes a set of information objects produced by an observing system. A hierarchical description of the contents of Product_Observational products appears below for raw and calibrated data products as an example:

Product_Observational

Identification_Area – attributes that identify and name an object

logical_identifier – a unique identifier urn:jaxa:darts:vco_rs:<collection>:<file_name_root>, e.g., urn:jaxa:darts:vco_rs:data_raw:rs_20160303_223100_udsc64_l1_rhcp

version_id – version of product

title – Short description of product used as the PDS4 search return

information_model_version – version of PDS4 information model used to create product

product_class – attribute provides the name of the product class (Product_Observational)

Observation_Area – attributes that provide information about the circumstances under which the data were collected.

Time_Coordinates – time attributes of data product

Primary_Results_Summary – high-level description of the types of products included in the collection or bundle

Investigation_Area – mission, observing campaign or other coordinated, large-scale data collection attributes

Observing_System – observing system attributes

Target_Identification – observation target attributes

Mission_Area – mission specific attributes needed to describe data product

Discipline_Area – discipline specific attributes needed to describe data product

File_Area_Observational – describes a file and one or more tagged_data_objects contained within.

File – identifies the file that contains one or more data objects

Table_Binary – binary table for Akatsuki RS Level 1 data

or

Table_Character – ASCII table for Akatsuki RS Level 2 / Level3 / Level 4 data

Information in the preceding paragraphs was distilled from the PDS4 Information Model provided by PDS. Additional information on product labels can be found at <https://pds.nasa.gov/datastandards/about/>.

The file naming conventions for the raw images, calibrated images, derived maps, and Geometry products are same for the four cameras, UVI, IR1, IR2, and LIR. In addition to the four cameras, the data of LAC and RS have very similar file naming conventions. In this section, the file naming conventions for the RS observations are described.

The filename has the format

Level 1/3/4: rs_{YYYY}{MM}{DD}_{hh}{mm}{ss}_{gs}_l{level}_v{ver}.{ext}

Level 2: rs_{YYYY}{MM}{DD}_{hh}{mm}{ss}_{gs}_l{level}_v{ver}.{ext}

where variables are denoted by string enclosed by the braces {}. The description of the variables is available in the following:

{YYYY}: year in four-digits

{MM}: zero-padded month in two digits from 01 to 12

{DD}: zero-padded day in two digits from 01 to 31

{hh}: zero-padded hour in two digits from 00 to 23

{mm}: zero-padded minute in two digits from 00 to 59

{ss}: zero-padded second in two digits from 00 to 60

Here the date and the time correspond to those of the start of recording at the ground station in UTC.

{gs}: abbreviated name for receiving ground station and antenna according to [Table 1](#)

{level}: data level of product (1 through 4)

{type}: type of data (Level 1, 3, and 4 only)

Level 1 only:

- rhcp: right-handed circularly polarized signal
- lhcp: left-handed circularly polarized signal

Level 3 only:

- i: data obtained during ingress
- e: data obtained during egress

Level 4 only:

- ai: atmospheric density, temperature and pressure profile obtained during ingress
- ae: atmospheric density, temperature and pressure profile obtained during egress
- pi: sulfuric acid mixing ratio profile obtained during ingress
- pe: sulfuric acid mixing ratio profile obtained during egress
- ii: electron density profile obtained during ingress
- ie: electron density profile data obtained during egress

Note that in the current release only Level 4 data of type ai and ae are available.

{ver}: version string of the product in two digits. The value is larger than or equal to 10

{ext}: extension of the file

- lbl: PDS3 label file
- lblx: PDS4 XML label file
- img: L1 binary file for K5/VSSP or K5/VSSP32 data
- prd: L1 binary file for CCSDS RDEF Product File
- tab: ASCII DSV file
- pdf: PDF file for browse product

3.5 Standards Used in Generating Data Products

3.5.1 PDS Standards

All data products described in this SIS conform to PDS4 standards as described in the PDS Standards document noted in the [“Applicable Documents” section](#) of this SIS. Prior to public release, all data products will have passed a PDS peer review to ensure compliance with applicable standards.

The Venus Climate Orbiter Akatsuki mission uses the 1.18.0.0 version or later of the PDS4 information model. All Venus Climate Orbiter Akatsuki Radio Science experiment products will conform to this standard, however products may have various versions of specific Discipline Dictionaries.

3.5.2 Time Standards

All Venus Climate Orbiter Akatsuki Radio Science experiment data products contain UTC times in their file names that have been derived from the Venus Climate Orbiter Akatsuki spacecraft clock time, TI. The transformation table from the spacecraft clock to UTC is provided by SIRIUS (Scientific Information Retrieval and Integrated Utilization System) and is converted to SPICE SCLK file by the Akatsuki SPICE and Data Archive (SPIDAr) team. The transformation from the spacecraft clock time to UTC time is conducted by the SPIDAr team proprietarily using the SPICE SCLK and LSK kernels and the SPICE toolkit. However, UTC time can be converted by users to other times using standard SPICE routines with the SPICE SCLK file included in the Venus Climate Orbiter Akatsuki SPICE Archive Bundle.

3.5.3 Coordinate Systems

3.5.3.1 Space

Some geometric quantities appearing in header data are in J2000 coordinates. In this coordinate, the +Z-axis points northward along the Earth's J2000 rotation axis and the +X-axis points toward the first point of Aries.

3.5.3.2 Venus

For the Venusian geometry, IAU Venus that is defined as the cytherocentric coordinate system for Venus is used. The defined ranges of the longitude and the latitude are from 0 to 360 and from -90 to 90, respectively. As a standard Venus radius 6051.8 km is assumed.

3.5.4 Data Storage Conventions

All Venus Climate Orbiter Akatsuki RS data products are stored as binary tables for raw data and as ASCII tables for calibrated and derived data.

3.6 Data Validation

The RS team checks the validity of the data manually and visually when calibrated and derived data products are created.

3.7 Data Quality and Coverage

During Akatsuki's Sun orbiting phase, solar corona observations were performed in 2011 during superior conjunction. Solar corona observations were also performed several times from Venus orbit during superior conjunction. For solar corona observations, only raw data (Level 1) is provided. Solar corona observations were recorded at the UDSC ground station and the IDSN ground station. An overview of the timeline of observations is found in the VCO Akatsuki mission event timeline document in the VCO Akatsuki mission bundle.

Geometry information such as the position of the spacecraft, Venus, and Earth is calculated using the SPICE toolkit and the SPICE kernels provided by the VCO Akatsuki SPICE Archive Bundle.

Recordings at the Weilheim station are done by a closed-loop receiver, unlike other stations where open-loop receivers are used. Since it takes time for the closed-loop receiver to capture the signal, only the ingress occultation is usually observed. The egress occultation is observed at a limited number of opportunities with good observation conditions.

A summary of radio occultations for Venus' atmosphere is given in [Table 4](#) and visualized for each calendar year in [Figure 3a-i](#).

Table 4: List of radio occultations for Venus' atmosphere

| Date/Time | Egress / Ingress | Orbit No. | Antenna | Longitude (deg) | Latitude (deg) | Local Time (hour) |
|------------------|------------------|-----------|---------|-----------------|----------------|-------------------|
| 2016-03-03T22:42 | Ingress | 9 | UDSC64 | 356.49 | -39.56 | 15.71 |
| 2016-03-03T23:22 | Egress | 9 | UDSC64 | 175.34 | -66.94 | 3.79 |
| 2016-03-24T21:43 | Ingress | 11 | UDSC64 | 53.13 | 0.17 | 16.21 |
| 2016-03-24T22:19 | Egress | 11 | UDSC64 | 232.83 | -36.11 | 4.24 |
| 2016-04-15T03:24 | Ingress | 13 | UDSC64 | 110.79 | 5.67 | 16.71 |
| 2016-04-15T03:53 | Egress | 13 | UDSC64 | 290.72 | -24.95 | 4.72 |
| 2016-04-26T00:34 | Ingress | 14 | UDSC64 | 140.33 | 6.53 | 16.96 |
| 2016-04-26T01:03 | Egress | 14 | UDSC64 | 320.36 | -19.94 | 4.97 |
| 2016-05-07T00:02 | Ingress | 15 | UDSC64 | 170.15 | 9.7 | 17.23 |
| 2016-05-07T00:33 | Egress | 15 | UDSC64 | 350.22 | -14.03 | 5.23 |
| 2016-05-18T01:55 | Ingress | 16 | UDSC64 | 200.28 | 15.29 | 17.49 |
| 2016-05-18T02:28 | Egress | 16 | UDSC64 | 20.28 | -7.26 | 5.50 |

| Date/Time | Egress / Ingress | Orbit No. | Antenna | Longitude (deg) | Latitude (deg) | Local Time (hour) |
|------------------|---------------------|--------------|------------------|-----------------|----------------|-------------------|
| 2016-07-12T07:11 | Ingress | 21 | UDSC64 | 351.25 | 45.33 | 18.83 |
| 2016-07-23T02:42 | Ingress | 22 | UDSC64 | 20.70 | 49.65 | 19.11 |
| 2016-07-23T03:11 | Egress | 22 | UDSC64 | 199.06 | 7.54 | 7.22 |
| 2017-02-06T01:48 | Ingress | 40 | UDSC64 | 178.97 | -25.01 | 1.21 |
| 2017-02-06T02:09 | Egress | 40 | UDSC64 | 13.82 | -73.10 | 12.22 |
| 2017-03-21T11:05 | Ingress | 44 | IDSN32 | 245.90 | -25.93 | 5.73 |
| 2017-03-21T11:22 | Egress | 44 | IDSN32 | 131.87 | -79.00 | 13.33 |
| 2017-05-04T19:48 | Ingress | 48 | UDSC64 | 309.98 | -50.05 | 10.58 |
| 2017-05-04T20:02 | Egress | 48 | UDSC64 | 238.28 | -77.21 | 15.37 |
| 2017-05-15T21:34 | Ingress | 49 | UDSC64 | 336.20 | -19.28 | 11.10 |
| 2017-05-15T22:00 | Egress | 49 | UDSC64 | 157.25 | -61.55 | 23.04 |
| 2017-05-26T21:05 | Ingress | 50 | UDSC64 | 1.87 | -0.65 | 11.63 |
| 2017-05-26T21:32 | Egress | 50 | UDSC64 | 181.19 | -47.46 | 23.68 |
| 2017-06-06T18:22 | Ingress | 51 | UDSC64 | 27.95 | 14.71 | 12.12 |
| 2017-06-06T18:47 | Egress | 51 | UDSC64 | 207.32 | -38.92 | 0.16 |
| 2017-07-09T06:20 | Ingress | 54 | IDSN32 | 109.6 | 34.23 | 13.32 |
| 2017-07-20T05:06 | Ingress | 55 | UDSC64 IDSN32 | 137.96 | 41.56 | 13.67 |
| 2017-07-20T05:35 | Egress | 55 | UDSC64 IDSN32 | 319.11 | -1.57 | 1.59 |
| 2017-07-31T06:17 | Ingress | 56 | IDSN32 | 166.23 | 56.78 | 14.05 |
| 2017-07-31T06:47 | Egress | 56 | IDSN32 | 348.42 | 15.48 | 1.90 |
| 2017-08-11T09:22 | Ingress | 57 | IDSN32 | 167.59 | 78.28 | 16.24 |
| 2017-08-11T09:44 | Egress | 57 | IDSN32 | 18.09 | 39.03 | 2.21 |
| 2018-02-03T01:10 | Ingress | 73 | UDSC64 | 315.73 | -22.56 | 18.51 |
| 2018-02-03T01:41 | Egress | 73 | UDSC64 | 133.80 | -58.23 | 6.64 |
| 2018-03-19T00:32 | Ingress | 77 | UDSC64 | 75.22 | -19.26 | 19.55 |
| 2018-03-19T01:04 | Egress | 77 | UDSC64 | 255.58 | -41.38 | 7.53 |
| 2018-03-30T04:05 | Ingress | 78 | UDSC64 IDSN32 | 105.46 | -11.51 | 19.82 |
| 2018-03-30T04:37 | Egress | 78 | UDSC64 IDSN32 | 286.09 | -32.53 | 7.79 |
| 2018-04-21T06:52 | Ingress | 80 | UDSC64 | 165.67 | 6.74 | 20.37 |

| Date/Time | Egress / Ingress | Orbit No. | Antenna | Longitude (deg) | Latitude (deg) | Local Time (hour) |
|------------------|---------------------|--------------|---------------------------|-----------------|----------------|-------------------|
| 2018-04-21T07:19 | Egress | 80 | UDSC64 | 346.04 | -17.98 | 8.35 |
| 2018-05-02T04:36 | Ingress | 81 | UDSC64 | 195.36 | 13.61 | 20.65 |
| 2018-05-02T05:02 | Egress | 81 | UDSC64 | 15.41 | -13.68 | 8.65 |
| 2018-05-13T00:28 | Ingress | 82 | UDSC64 | 224.74 | 18.58 | 20.93 |
| 2018-06-14T14:07 | Ingress | 85 | IDSN32 | 312.31 | 34.65 | 21.83 |
| 2018-06-14T14:49 | Egress | 85 | IDSN32 | 130.66 | 8.96 | 9.95 |
| 2018-06-25T14:29 | Ingress | 86 | IDSN32 | 341.72 | 46.59 | 22.15 |
| 2018-06-25T15:19 | Egress | 86 | IDSN32 | 159.35 | 23.56 | 10.31 |
| 2019-01-31T11:24 | Ingress | 106 | WHM30 | 79.53 | 36.27 | 12.82 |
| 2019-05-10T00:38 | Ingress | 115 | IDSN32 | 341.66 | -13.89 | 15.53 |
| 2019-05-10T01:06 | Egress | 115 | IDSN32 | 161.63 | 4.16 | 3.54 |
| 2019-05-21T01:04 | Ingress | 116 | UDSC64 IDSN32 | 11.35 | -18.69 | 15.80 |
| 2019-05-21T01:35 | Egress | 116 | UDSC64 IDSN32 | 191.29 | -3.07 | 3.81 |
| 2019-06-12T07:11 | Ingress | 118 | UDSC64 | 71.22 | -33.43 | 16.38 |
| 2019-07-04T11:10 | Ingress | 120 | IDSN32 WHM30 | 130.62 | -46.42 | 16.98 |
| 2019-07-04T11:40 | Egress | 120 | IDSN32 | 311.53 | -24.24 | 4.92 |
| 2019-07-26T05:52 | Ingress | 122 | UDSC64 IDSN32 WHM30 | 188.80 | -56.80 | 17.60 |
| 2019-07-26T06:24 | Egress | 122 | UDSC64 IDSN32 | 10.61 | -21.09 | 5.49 |
| 2020-02-09T02:19 | Ingress | 140 | UDSC64 | 6.93 | -8.83 | 22.37 |
| 2020-02-09T02:50 | Egress | 140 | UDSC64 | 186.76 | 25.80 | 10.39 |
| 2020-02-20T00:52 | Ingress | 141 | UDSC64 | 35.38 | -19.69 | 22.73 |
| 2020-02-20T01:19 | Egress | 141 | UDSC64 | 215.4 | 20.47 | 10.74 |
| 2020-03-12T16:38 | Ingress | 143 | WHM30 | 89.81 | -33.78 | 23.58 |
| 2020-03-23T12:27 | Ingress | 144 | WHM30 | 115.73 | -40.4 | 0.1 |
| 2020-04-03T10:03 | Ingress | 145 | UDSC64 WHM30 | 139.78 | -51.17 | 0.75 |
| 2020-04-03T10:29 | Egress | 145 | UDSC64 WHM30 | 326.96 | -12.96 | 12.28 |
| 2020-04-14T10:11 | Ingress | 146 | UDSC64 IDSN32 WHM30 | 156.92 | -69.28 | 1.89 |

| Date/Time | Egress / Ingress | Orbit No. | Antenna | Longitude (deg) | Latitude (deg) | Local Time (hour) |
|------------------|---------------------|--------------|---------------------------|-----------------|----------------|-------------------|
| 2020-04-14T10:33 | Egress | 146 | UDSC64 IDSN32 WHM30 | 355.27 | -35.57 | 12.67 |
| 2020-05-28T20:56 | Ingress | 150 | UDSC64 | 239.82 | -64.27 | 5.51 |
| 2020-05-28T21:22 | Egress | 150 | UDSC64 | 66.81 | -28.31 | 17.05 |
| 2020-06-08T19:48 | Ingress | 151 | UDSC64 | 254.65 | 46.7 | 6.76 |
| 2020-06-08T20:15 | Egress | 151 | UDSC64 | 74.92 | -7.23 | 18.75 |
| 2020-07-22T05:12 | Ingress | 155 | UDSC64 IDSN32 WHM30 | 327.97 | -39.18 | 10.74 |
| 2020-07-22T05:43 | Egress | 155 | IDSN32 WHM30 | 144.63 | -7.8 | 22.97 |
| 2020-08-02T04:48 | Ingress | 156 | UDSC64 WHM30 | 353.35 | -45.24 | 11.29 |
| 2020-08-02T05:24 | Egress | 156 | UDSC64 | 168.93 | -19.89 | 23.59 |
| 2020-08-13T06:37 | Ingress | 157 | IDSN32 | 20.75 | -56.37 | 11.73 |
| 2020-08-13T07:13 | Egress | 157 | IDSN32 | 194.69 | -34.92 | 0.14 |
| 2020-08-24T09:49 | Ingress | 158 | WHM30 | 53.32 | -76.45 | 11.84 |
| 2020-08-24T10:14 | Egress | 158 | WHM30 | 220.86 | -56.54 | 0.68 |
| 2021-01-04T07:42 | Ingress | 170 | IDSN32 WHM30 | 38.03 | 51.35 | 16.21 |
| 2021-01-04T08:23 | Egress | 170 | IDSN32 WHM30 | 219.81 | 65.22 | 4.17 |
| 2021-01-15T07:31 | Ingress | 171 | WHM30 | 69.15 | 26.54 | 16.46 |
| 2021-01-15T08:13 | Egress | 171 | WHM30 | 249.88 | 46.83 | 4.41 |
| 2021-02-06T03:23 | Ingress | 173 | UDSC64 | 129.02 | 3.49 | 16.93 |
| 2021-02-06T03:54 | Egress | 173 | UDSC64 | 309.56 | 32.64 | 4.90 |
| 2021-04-24T22:41 | Ingress | 180 | UDSC64 | 341.09 | -7.29 | 18.71 |
| 2021-04-24T23:12 | Egress | 180 | UDSC64 | 161.19 | 3.25 | 6.71 |
| 2021-05-05T23:46 | Ingress | 181 | UDSC64 | 10.97 | -10.53 | 19.00 |
| 2021-06-18T16:39 | Ingress | 185 | WHM30 | 128.53 | -28.01 | 20.20 |
| 2021-06-18T17:33 | Egress | 185 | WHM30 | 309.85 | -11.77 | 8.12 |
| 2021-06-29T18:46 | Ingress | 186 | WHM30 | 158.00 | -36.86 | 20.52 |
| 2021-06-29T19:22 | Egress | 186 | WHM30 | 339.93 | -22.13 | 8.40 |
| 2021-07-10T19:22 | Ingress | 187 | WHM30 | 187.52 | -47.69 | 20.84 |

| Date/Time | Egress / Ingress | Orbit No. | Antenna | Longitude (deg) | Latitude (deg) | Local Time (hour) |
|------------------|---------------------|--------------|------------------|-----------------|----------------|-------------------|
| 2021-09-26T14:19 | Ingress | 194 | IDSN32 WHM30 | 35.89 | -4.86 | 22.91 |
| 2021-09-26T17:16 | Egress | 194 | WHM30 | 215.62 | -5.97 | 10.95 |
| 2021-11-21T06:52 | Ingress | 199 | UDSC64 IDSN32 | 174.39 | -4.68 | 1.07 |
| 2021-11-21T07:45 | Egress | 199 | UDSC64 IDSN32 | 353.11 | -14.62 | 13.16 |
| 2021-12-02 | Egress | 200 | IDSN32 | 17.01 | -19.57 | 13.85 |
| 2021-12-13 | Ingress | 201 | IDSN32 | 218.88 | -2.55 | 2.66 |
| 2021-12-13 | Egress | 201 | IDSN32 | 38.21 | -23.77 | 14.71 |
| 2021-12-24 | Ingress | 202 | IDSN32 | 235.19 | 0.76 | 3.83 |
| 2021-12-24 | Egress | 202 | IDSN32 | 55.64 | -28.43 | 15.80 |
| 2022-01-04T06:17 | Ingress | 203 | UDSC64 | 246.86 | 0.40 | 5.30 |
| 2022-01-04T07:05 | Egress | 203 | UDSC64 | 69.42 | -36.12 | 17.14 |
| 2022-01-15T04:42 | Ingress | 204 | UDSC64 | 255.24 | -12.64 | 7.00 |
| 2022-01-15T05:15 | Egress | 204 | UDSC64 | 83.25 | -49.86 | 18.47 |
| 2022-03-12T00:12 | Ingress | 209 | UDSC64 IDSN32 | 357.78 | -26.21 | 11.71 |
| 2022-03-12T00:42 | Egress | 209 | UDSC64 IDSN32 | 183.61 | -54.35 | 23.32 |
| 2022-03-23T03:09 | Ingress | 210 | UDSC64 IDSN32 | 26.24 | -8.84 | 12.09 |
| 2022-03-23T03:39 | Egress | 210 | UDSC64 IDSN32 | 208.33 | -39.60 | 23.96 |
| 2022-04-03T03:39 | Ingress | 211 | UDSC64 | 54.42 | 4.06 | 12.48 |
| 2022-04-03T04:05 | Egress | 211 | UDSC64 | 235.10 | -30.59 | 0.43 |
| 2022-04-24T23:41 | Ingress | 213 | UDSC64 IDSN32 | 110.64 | 16.28 | 13.20 |
| 2022-04-25T00:04 | Egress | 213 | UDSC64 IDSN32 | 290.67 | -21.03 | 1.20 |
| 2022-05-05T21:47 | Ingress | 214 | UDSC64 | 139.08 | 18.96 | 13.53 |
| 2022-05-05T22:11 | Egress | 214 | UDSC64 | 319.15 | -15.28 | 1.53 |
| 2022-05-16T21:39 | Ingress | 215 | UDSC64 | 167.88 | 23.66 | 13.86 |
| 2022-05-16T22:07 | Egress | 215 | UDSC64 | 348.13 | -6.88 | 1.84 |
| 2022-05-27T23:57 | Ingress | 216 | UDSC64 IDSN32 | 197.04 | 32.36 | 14.18 |
| 2022-05-28T00:28 | Egress | 216 | UDSC64 IDSN32 | 17.63 | 4.42 | 2.13 |

| Date/Time | Egress / Ingress | Orbit No. | Antenna | Longitude (deg) | Latitude (deg) | Local Time (hour) |
|------------------|---------------------|--------------|-----------------|-----------------|----------------|-------------------|
| 2022-06-08T04:29 | Ingress | 217 | UDSC64 WHM30 | 226.48 | 45.52 | 14.50 |
| 2022-06-08T05:02 | Egress | 217 | UDSC64 WHM30 | 47.54 | 18.47 | 2.44 |
| 2022-12-13T08:48 | Ingress | 234 | IDSN32 WHM30 | 19.03 | -45.42 | 19.06 |
| 2022-12-13T09:03 | Egress | 234 | IDSN32 WHM30 | 90.26 | -88.20 | 14.32 |
| 2023-02-07T03:24 | Ingress | 239 | UDSC64 | 169.87 | 5.42 | 20.41 |
| 2023-02-07T03:57 | Egress | 239 | UDSC64 | 349.65 | -30.74 | 8.43 |
| 2023-02-18T06:35 | Ingress | 240 | UDSC64 | 200.14 | 18.65 | 20.68 |
| 2023-02-18T07:04 | Egress | 240 | UDSC64 | 20.19 | -22.61 | 8.68 |
| 2023-03-01T07:13 | Ingress | 241 | UDSC64 | 230.31 | 29.68 | 20.93 |
| 2023-03-01T07:39 | Egress | 241 | UDSC64 | 50.24 | -18.11 | 8.94 |
| 2023-03-12T05:40 | Ingress | 242 | UDSC64 | 260.39 | 38.07 | 21.18 |
| 2023-03-12T06:05 | Egress | 242 | UDSC64 | 79.88 | -15.45 | 9.22 |
| 2023-03-23T03:08 | Ingress | 243 | UDSC64 | 290.48 | 44.83 | 21.42 |
| 2023-03-23T03:34 | Egress | 243 | UDSC64 | 109.14 | -9.96 | 9.51 |
| 2023-04-03T01:08 | Ingress | 244 | UDSC64 | 320.94 | 52.94 | 21.65 |
| 2023-04-03T01:35 | Egress | 244 | UDSC64 | 137.90 | 3.06 | 9.86 |
| 2024-01-05T09:32 | Ingress | 269 | WHM30 | 205.30 | -52.13 | 14.44 |
| 2024-01-05T10:08 | Egress | 269 | WHM30 | 27.72 | -57.42 | 2.29 |
| 2024-01-16T11:28 | Ingress | 270 | WHM30 | 236.00 | -30.25 | 14.68 |
| 2024-01-16T12:05 | Egress | 270 | WHM30 | 56.91 | -40.05 | 2.63 |
| 2024-02-18T06:53 | Ingress | 273 | WHM30 | 325.45 | -2.02 | 15.45 |
| 2024-03-11T05:31 | Ingress | 275 | IDSN32 WHM30 | 25.18 | -5.79 | 15.95 |
| 2024-03-11T05:58 | Egress | 275 | IDSN32 WHM30 | 204.99 | -22.28 | 3.97 |
| 2024-03-22T08:19 | Ingress | 276 | IDSN32 WHM30 | 55.42 | -6.75 | 16.21 |
| 2024-04-24T23:52 | Ingress | 279 | UDSC64 | 146.68 | 1.17 | 17.00 |

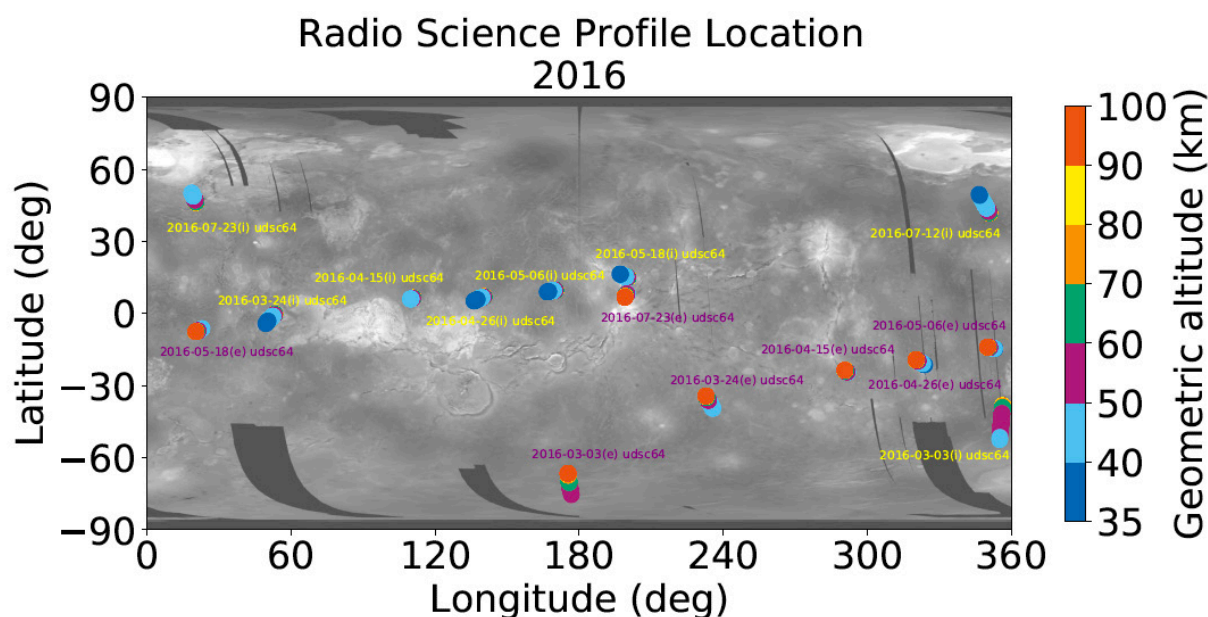


Figure 3a: Tangent point locations of radio occultations during year 2016 for which Level 4 data were derived. Labels give the date and antenna used for each occultation, with ingress measurements in yellow and egress measurements in purple. Note that in some instances, occultation opportunities were recorded with multiple antennas. Ingress measurements have the lowest tangent altitude on top while egress measurements have the highest tangent altitude on top. The topographic map underlying the figure is derived from Magellan data (version 2, 1997 release, [Ford, 1992](#)).

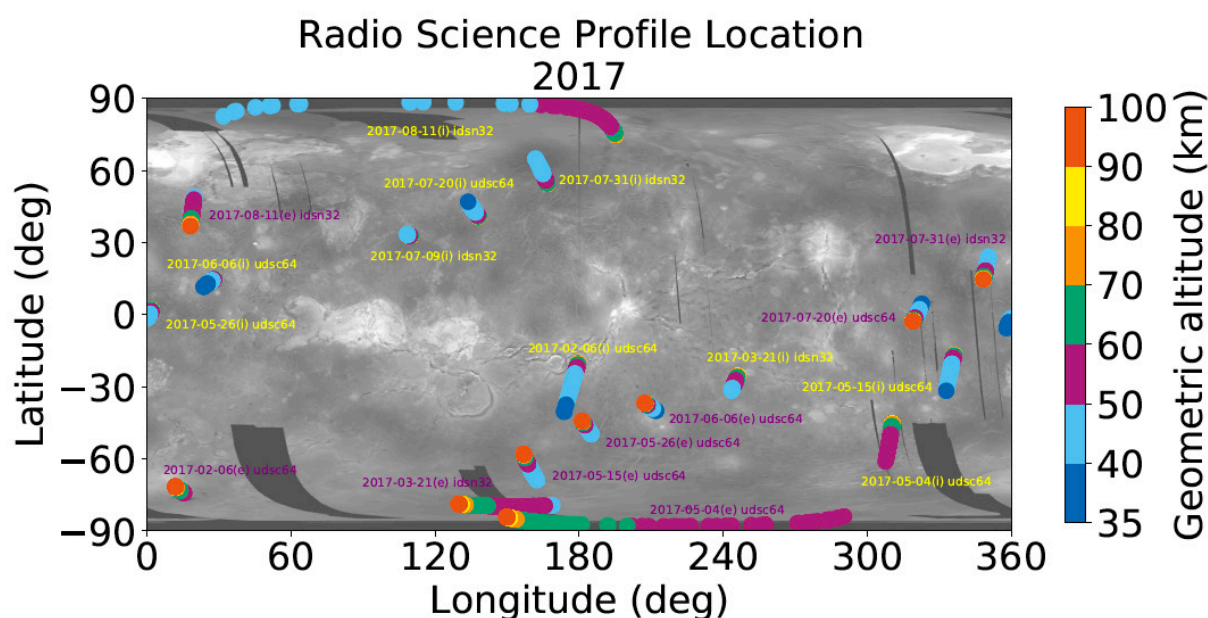


Figure 3b: As [Figure 3a](#) but for radio occultations during 2017.

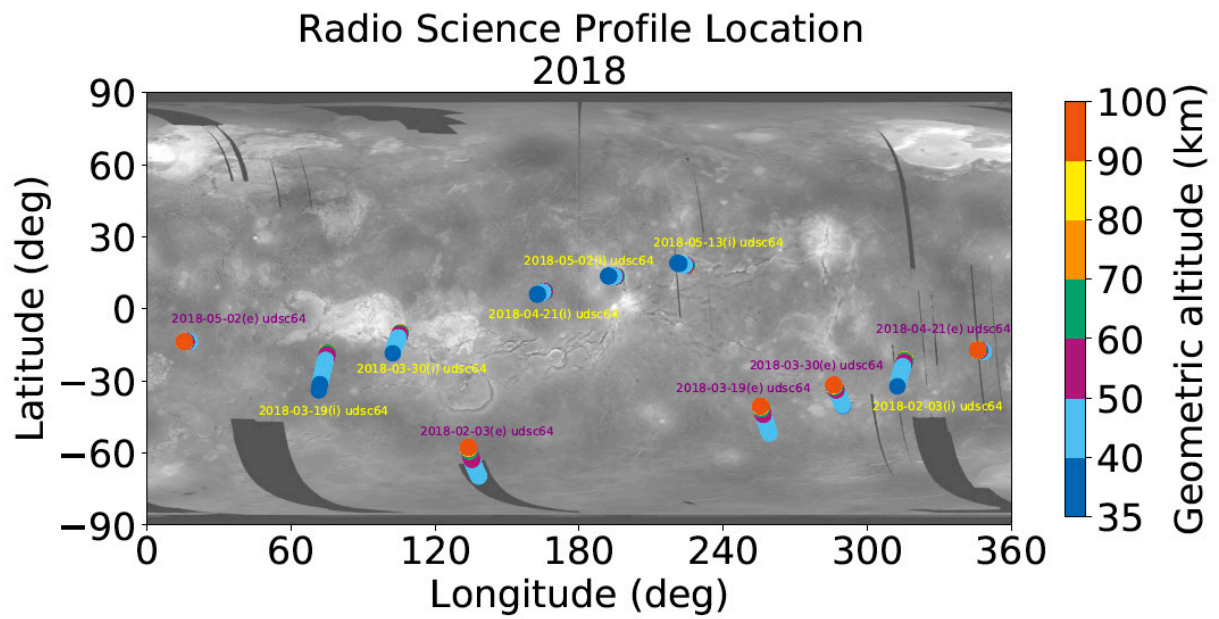


Figure 3c: As [Figure 3a](#) but for radio occultations during 2018.

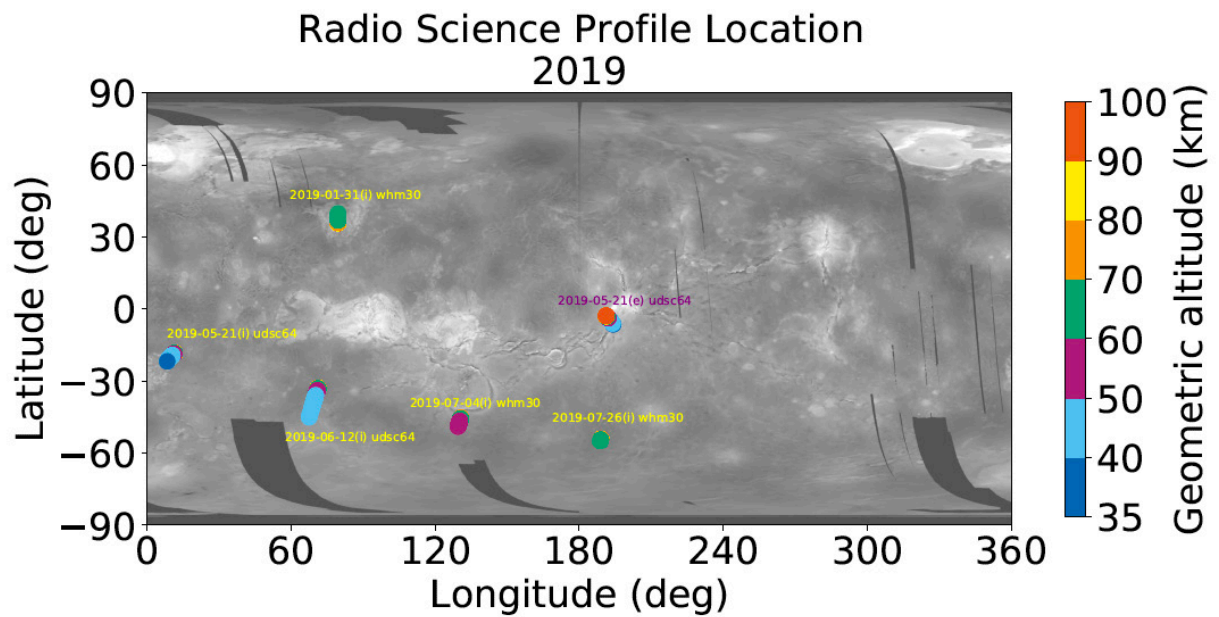


Figure 3d: As [Figure 3a](#) but for radio occultations during 2019.

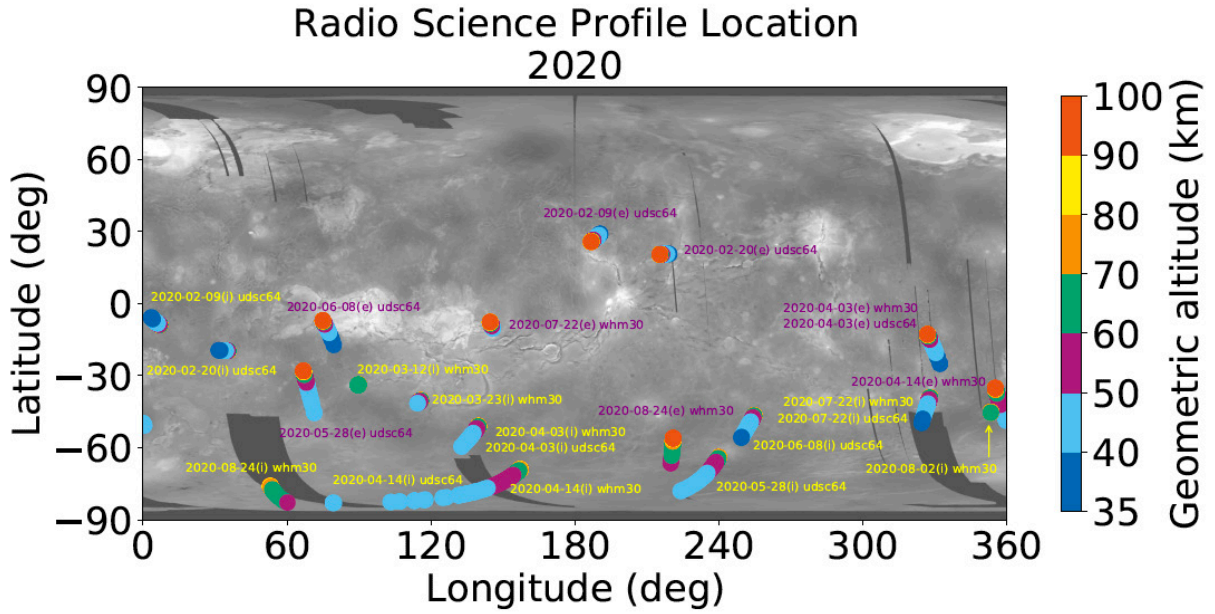


Figure 3e: As Figure 3a but for radio occultations during 2020.

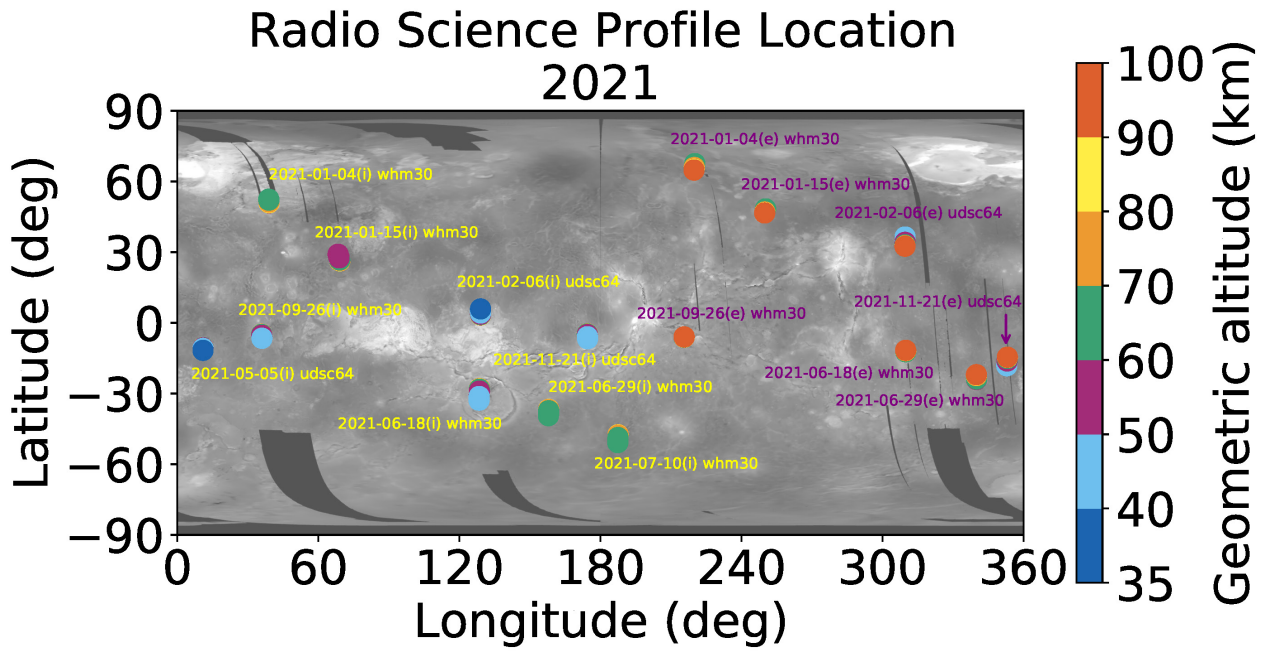


Figure 3f: As Figure 3a but for radio occultations during 2021.

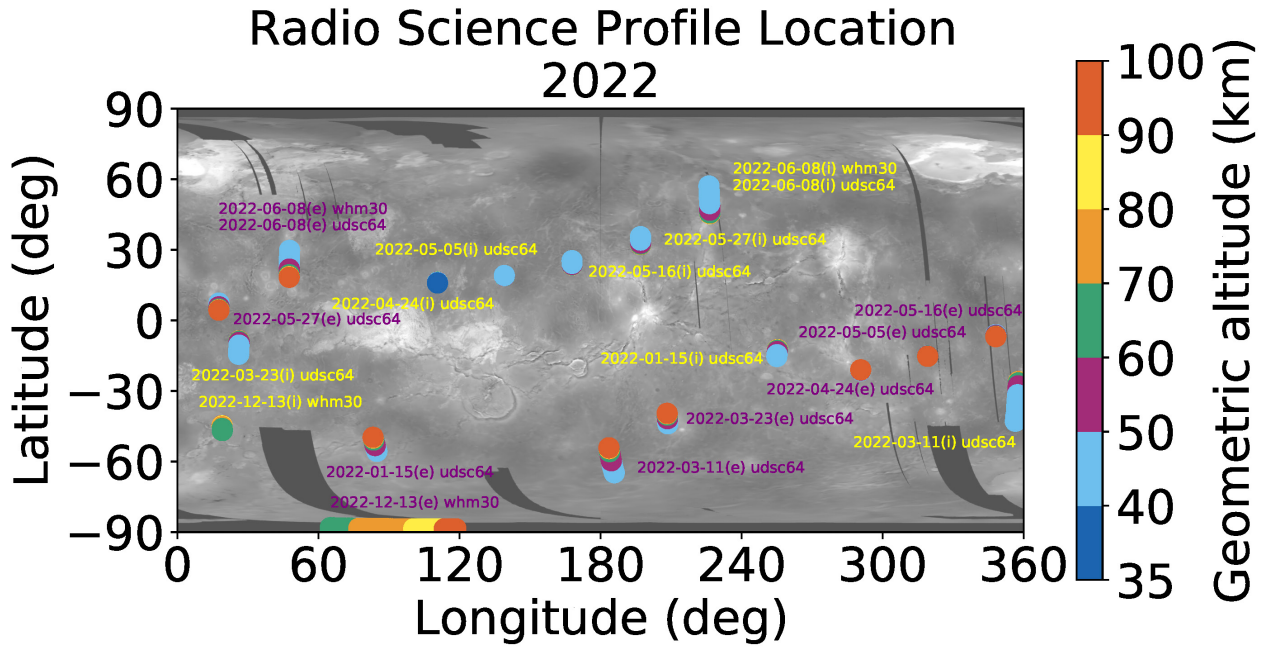


Figure 3g: As [Figure 3a](#) but for radio occultations during 2022.

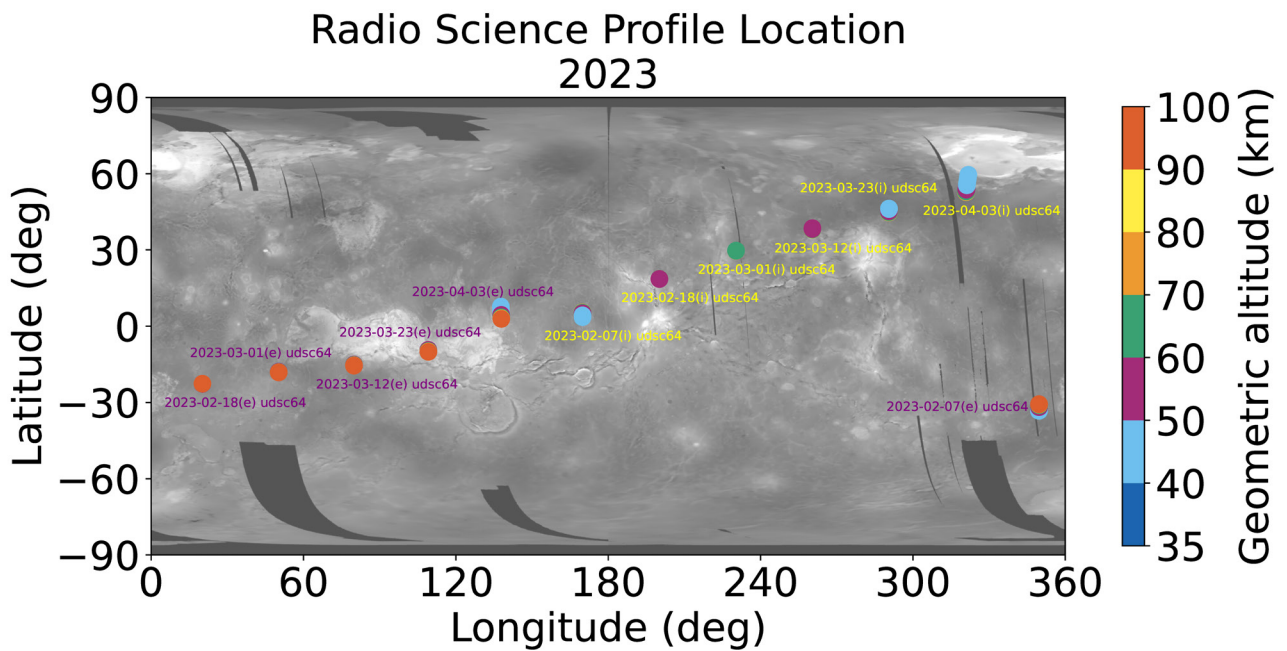


Figure 3h: As [Figure 3a](#) but for radio occultations during 2023.

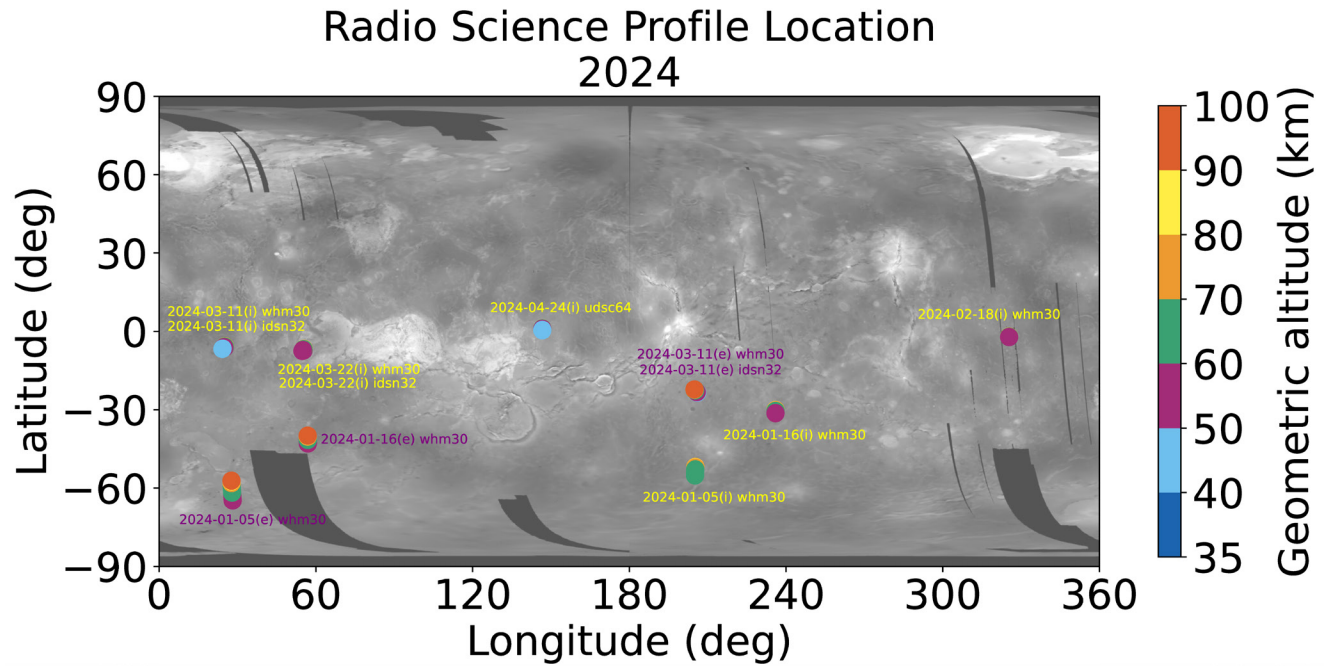


Figure 3i: As Figure 3a but for radio occultations during 2024.

4 Detailed Data Product Specifications

The following sections provide detailed data product specifications for each level of the RS data product.

4.1 Data Product Structure and Organization

The Venus Climate Orbiter data archive is organized as bundles by instrument/investigation. The RS bundle of the archive is organized by data collection and processing level. The list of collections and products in each collection is summarized in Table 5. These collections are under the Venus Climate Orbiter Akatsuki RS bundle directory, *vco_rs*. Each name of collection is the same as the directory name in the bundle.

Table 5: List of collections and products in each collection

| Directory name of collection | Collection | Products in the collection |
|------------------------------|-------------------------------|---|
| browse | RS Browse Collection | RS Level 4 Browse Product |
| data_raw | RS Raw Data Collection | RS Raw (Level 1) Data Product |
| data_calibrated | RS Calibrated Data Collection | RS Calibrated (Level 2) Data Product |
| data_derived | RS Derived Data Collection | RS Derived (Level 3/4) Data Product |
| document | RS Document Collection | SIS (This file) and relevant documents/papers |
| miscellaneous | RS Miscellaneous Collection | RS Venus atmosphere observation summary product |

4.2 Data Format Descriptions

4.2.1 Level 1 - Raw Data

RS Level 1 data are raw signal intensity measurements of Akatsuki X-band radio occultation observations as received by the ground station. Raw data from the UDSC and ISDN stations are open-loop recordings. Data from these stations are provided in binary format and come with PDS4-compliant detached XML labels.

For data received by the UDSC station, files containing Venus observations up to and including year 2020 as well as files containing solar corona observations from 2011 are provided in K5/VSSP format, corresponding to the 8-byte structure as described by [Kondo \(2010\)](#). Files containing Venus observations from the UDSC station from 2021 onwards are provided in K5/VSSP32 format ([Kondo 2010](#)). Files containing solar observations from the UDSC station from 2016 onwards and files from the ISDN station are provided in CCSDS Delta-DOR Raw Data Exchange Format (RDEF) Product File ([CCSDS 2013](#)).

For all raw data formats (K5/VSSP, K5VSSP32, and CCSDS Delta-DOR RDEF Product File) sampler output is made up of multiple frames, each consisting of a header and a data block. Each header and data block combination forms a record that covers 1 second worth of data ([Figure 4](#)). For each radio occultation, a series of records is provided in order to cover the occultation duration. The number of records will hence vary.

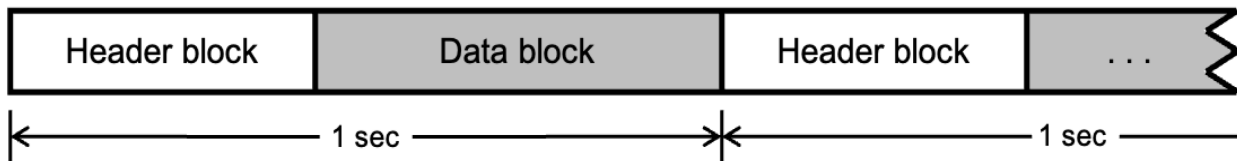


Figure 4: Basic data structure for the K5/VSSP, K5VSSP32, and CCSDS Delta-DOR RDEF Product File formats. Header blocks and data blocks alternate. A header block together with its corresponding data block cover one second of data.

A header block of K5/VSSP data consists of 8-byte data which contain two sync blocks, time information, and sampling parameters (see Section 2.1 in [Kondo \(2010\)](#)). A header block of K5/VSSP32 data consists of 32-byte data which contain similar parameters as K5/VSSP as well as additional parameters (see Sections 2.2 and 2.3.2 “Format #1” in [Kondo \(2010\)](#)). The second sync pattern can be used to distinguish between K5/VSSP and K5/VSSP32 formats, it is 0x8B for VSSP but 0x8C for VSSP32. [Table 6](#) and [Table 8](#) give the structure of header data of L1 binary records in K5/VSSP format. The header section contains three fields ([Table 6](#)), the second of which in turn contains packed data fields in a predetermined bit structure ([Table 8](#)). [Table 7](#), [Table 8](#), [Table 9](#), and [Table 10](#) provide the same information for K5/VSSP32 format. In this format the header section contains 8 fields ([Table 7](#)), three of which contain packed data fields. The first packed data field is identical with the one in VSSP format ([Table 8](#)), the structures of the other two are given in [Table 9](#) and [Table 10](#).

Table 6: Structure of header data of RS Level 1 binary records in K5/VSSP format.

| Field no. | Name | Location (byte) | Data type | Length (byte) | Description |
|-----------|---|-----------------|-------------------|---------------|--|
| 1 | First Sync Pattern | 1 | UnsignedLSB4 | 4 | First sync pattern indicating start of header. The value is always 0xFFFFFFFF. |
| 2 | Time, Sampling frequency, and A/D conversion bits | 5 | UnsignedBitString | 3 | Time, Sampling frequency, and A/D conversion bits. |
| | Packed data fields: 4-bit fields (see Table 8) | | | | |
| 3 | Second Sync Pattern | 8 | UnsignedByte | 1 | Second sync pattern indicating end of header. The value is always 0x8B. |

Table 7: Structure of header data of RS Level 1 binary records in K5/VSSP32 format.

| Field no. | Name | Location (byte) | Data type | Length (byte) | Description |
|-----------|---|-----------------|-------------------|---------------|--|
| 1 | First Sync Pattern | 1 | UnsignedLSB4 | 4 | First sync pattern indicating start of header. The value is always 0xFFFFFFFF. |
| 2 | Time, Sampling frequency, and A/D conversion bits | 5 | UnsignedBitString | 3 | Time, Sampling frequency, and A/D conversion bits. |
| | Packed data field 1: 4-bit fields (see Table 8) | | | | |
| 3 | Second Sync Pattern | 8 | UnsignedByte | 1 | Second sync pattern. The value is always 0x8C. |
| 4 | Day of year, Year, and Error flag for a previous frame | 9 | UnsignedBitString | 2 | Day of year, Year, and Error flag for a previous frame. |
| | Packed data field 2: 3-bit fields (see Table 9) | | | | |
| 5 | Auxiliary field size | 11 | UnsignedByte | 1 | Size of auxiliary field in bytes. |
| 6 | Version of VSSP32 control ROM | 12 | UnsignedBitString | 1 | Version of VSSP32 control ROM. |
| | Packed data field 3: 2-bit fields (see Table 10) | | | | |
| 7 | Auxiliary field format | 13 | UnsignedByte | 1 | Format of auxiliary field. |
| 8 | Auxiliary field | 14 | UnsignedByte | 19 | Auxiliary field. |

Table 8: Structure of packed data field 1 in header data Level 1 binary records in K5/VSSP and K5/VSSP32 formats.

| Field no. | Name | Start bit location | Stop bit location | Data type | Unit | Description |
|-----------|--------------------------------|--------------------|-------------------|-------------------|------|---|
| 1 | Time | 1 | 17 | UnsignedBitString | s | Time in seconds from 00:00 UTC. |
| 2 | Channel | 18 | 18 | UnsignedBitString | n/a | Number of channels used; 0 for 1ch, and 1 for 4ch. |
| 3 | Sampling Frequency | 19 | 22 | UnsignedBitString | n/a | Sampling frequency of recorded data ¹⁾ |
| 4 | A/D conversion resolution bits | 23 | 24 | UnsignedBitString | n/a | Number of analog-digital conversion resolution bits ²⁾ |

¹⁾ Sampling frequency of recorded data: 0 is for 40 kHz, 1:100 kHz, 2 is for 200 kHz, 3 is for 500 kHz, 4 is for 1 MHz, 5 is for 2 MHz, 6 is for 4 MHz, 7 is for 8 MHz, 8 is for 16 MHz, 9 is for 32 MHz, 10 is for 64 MHz, 11 is for 128 MHz, 12 is for 256 MHz, 13 is for 512 MHz, 14 is for 1024 MHz, and 15 is for 2048 MHz.

²⁾ Number of analog-digital conversion resolution bits: 0 is for 1 bit, 1 is for 2 bits, 2 is for 4 bits, and 3 is for 8 bits.

Table 9: Structure of packed data field 2 in header data Level 1 binary records in K5/VSSP32 format.

| Field no. | Name | Start bit location | Stop bit location | Data type | Unit | Description |
|-----------|-------------|--------------------|-------------------|-------------------|------|---|
| 1 | Day of year | 1 | 9 | UnsignedBitString | day | Day of year. |
| 2 | Year | 10 | 15 | UnsignedBitString | yr | Lower 2 digits of year from 00 to 63, that represents year from 2000 to 2063. |
| 3 | Error flag | 16 | 16 | UnsignedBitString | n/a | Error flag for a previous frame. |

Table 10: Structure of packed data field 3 in header data Level 1 binary records in K5/VSSP32 format.

| Field no. | Name | Start bit location | Stop bit location | Data type | Description |
|-----------|---------------|--------------------|-------------------|-------------------|----------------|
| 1 | Minor version | 1 | 4 | UnsignedBitString | Minor version. |
| 2 | Major version | 5 | 8 | UnsignedBitString | Major version. |

For the data output in both the K5/VSSP and K5/VSSP32 formats the 1 channel \times 8 bit pattern is used throughout the dataset (see Section 3.1 in [Kondo \(2010\)](#)). [Table 11](#) provides the structure of the data section of L1 binary records in both the K5/VSSP and K5/VSSP32 formats from the UDSC station. Data is organized in a data block group, each of which in turn contains a single subgroup with samples of 4-byte units. While the subgroup contains only one field type, the four repetitions of the field within the subgroup make up the 4-byte sample, reflecting the 1 channel \times 8 bit pattern (see Table 10 in [Kondo \(2010\)](#)). Note that the sampling frequency for Venus occultations is 4 MHz, leading to data block groups with 1000000 repetitions and a group length of 4000000 bytes, while the sampling frequency of solar occultations is 500 kHz, leading to data block groups with 125000 repetitions and a group length of 500000 bytes.

Table 11: Structure of the data section in Level 1 binary records in K5/VSSP and K5/VSSP32 formats.

| Group no. | | Name | Group location (byte) | Repetitions | Group length (byte) | Description | |
|-----------|---|------------------------|-----------------------|-----------------------|-----------------------|--|--|
| 1 | | Data Block | 9 ¹⁾ | 1000000 ²⁾ | 4000000 ²⁾ | Data block for 1 ch, 4 MHz of sampling frequency, and 8 bit for A/D conversion resolution. ²⁾ | |
| | 1 | Samples of 4-byte unit | 1 | 4 | 4 | Samples of 4 byte unit for 1 ch and 8 bit for A/D conversion resolution. | |
| | | Field no. | Name | Location (byte) | Data type | Length (byte) | Description |
| | | 1 | Sample | 1 | UnsignedByte | 1 | Sample for 1 ch and 8 bit for A/D conversion resolution. |

¹⁾ Information given for K5/VSSP. Group location for K5/VSSP32 is byte 33.

²⁾ Information given for occultations yielding atmospheric observations of Venus with 1 ch, 8 bit for A/D conversion resolution, and 4MHz of sampling frequency. Solar observations are sampled in data blocks for 1 ch, 500kHz of sampling frequency, giving 125000 repetitions and a group length of 500000 bytes.

Files from the IDSN station and files on solar corona observation after 2016 from the Usuda station are provided in CCSDS Delta-DOR Raw Data Exchange Format (RDEF) (CCSDS 2013). Delta-DOR RDEF relies on two types of files: an Observation File made of a sequence of ASCII text lines and a Product File made of a sequence of binary data records. For data provided in this bundle the content of the Observation File is included in the PDS4-compliant detached XML labels. The Product File is provided as is. Throughout the dataset, 8-bit samples are used (see Section 5 and Figure 5.2 in CCSDS (2013)).

Table 12 gives the structure of the header block of L1 binary records provided in Delta-DOR RDEF Product File. The header block consists of 21 fields distributed over 176 bytes. Note that entries between byte locations 97 and 172 are currently not used and their structure is not defined. The end label is hence found at byte location 173.

Table 12: Structure of header data of RS Level 1 binary records in Delta-DOR RDEF Product File

| Field no. | Name | Location (byte) | Data type | Length (byte) | Unit | Description |
|-----------|-------------------|-----------------|--------------|---------------|------|--|
| 1 | RECORD LABEL | 1 | ASCII_String | 4 | n/a | ASCII sequence needed to identify data type. The value is always 'RDEF'. |
| 2 | RECORD LENGTH | 5 | UnsignedLSB4 | 4 | byte | Indicates the length, in bytes, of the entire Record. ¹⁾ |
| 3 | RECORD VERSION ID | 9 | UnsignedLSB2 | 2 | n/a | Version number of the data record structure (=1 for the current version). The version number shall be synchronised with the one given in the Observation File. |
| 4 | STATION ID | 11 | UnsignedLSB2 | 2 | n/a | Internal network identifier for the station. |
| 5 | SPACECRAFT ID | 13 | UnsignedLSB2 | 2 | n/a | Internal network identifier for the spacecraft. |

| Field no. | Name | Location (byte) | Data type | Length (byte) | Unit | Description |
|-----------|---------------------------------------|-----------------|------------------|---------------|------|---|
| 6 | SAMPLE SIZE | 15 | UnsignedLSB2 | 2 | n/a | Specifies the resolution of the data samples contained in this data record. The value shall be 1, 2, 4, 8, or 16. |
| 7 | SAMPLE RATE | 17 | UnsignedLSB4 | 4 | Hz | Specifies the sample rate of the data contained in this record, in complex samples per second. ²⁾ |
| 8 | VALIDITY FLAG | 21 | UnsignedLSB2 | 2 | n/a | Contains a value to indicate whether an error was detected during recording. The value 0 shall mean no error (or no check was performed). A positive value is an implementation dependent error code. |
| 9 | AGENCY FLAG | 23 | UnsignedLSB2 | 2 | n/a | Specifies the Agency creating the file. The value 0 shall mean that this field is not in use. 1 = ESA, 2 = JAXA, 3 = NASA. |
| 10 | RF_TO_IF DOWNCONV | 25 | IEEE754LSBDouble | 8 | Hz | First downconversion stage: from RF to IF. Resolution: 1 Hz. ³⁾ |
| 11 | IF_TO_CHANNEL DOWNCONV | 33 | IEEE754LSBDouble | 8 | Hz | Second downconversion stage: from IF to channel center frequency. Resolution: 1 micro-Hz. ⁴⁾ |
| 12 | TIME TAG YEAR | 41 | UnsignedLSB2 | 2 | yr | Specifies the ST year of the data contained in the record. |
| 13 | TIME TAG DOY | 43 | UnsignedLSB2 | 2 | day | Specifies the ST DOY of the data contained in the record. |
| 14 | TIME TAG SECOND OF DAY | 45 | UnsignedLSB4 | 4 | s | Specifies the ST SOD of the data contained in the record. |
| 15 | TIME TAG PICOSECONDS OF THE SECOND | 49 | IEEE754LSBDouble | 8 | ps | Specifies the ST picoseconds of the second of the first sample contained in the record. A positive non-zero value is used when there is a known delay between the time of the first data sample and the beginning of the second one. Set to 0 if unknown. |
| 16 | CHANNEL ACCUMULATED PHASE | 57 | IEEE754LSBDouble | 8 | n/a | The value of the accumulated whole turns of the channel variable downconverter represented by the phase polynomial coefficients (Expressed in 'turns', i.e., $\text{rad}/(2\pi)$). ⁵⁾ |
| 17 | CHANNEL PHASE POLYNOMIAL COEFFICIENT0 | 65 | IEEE754LSBDouble | 8 | n/a | The channel phase polynomial coefficient of degree 0 (expressed in $\text{rad}/(2\pi)$). This item has to be referred to the second boundary, |

| Field no. | Name | Location (byte) | Data type | Length (byte) | Unit | Description |
|-----------|---------------------------------------|-----------------|------------------|---------------|------|---|
| | | | | | | as provided by item TIME TAG SECOND OF DAY. ⁶⁾ |
| 18 | CHANNEL PHASE POLYNOMIAL COEFFICIENT1 | 73 | IEEE754LSBDouble | 8 | n/a | The channel phase polynomial coefficient of degree 1 (expressed in $\text{rad}/(2\pi)/\text{s}$). This item has to be referred to the second boundary, as provided by item TIME TAG SECOND OF DAY. ⁶⁾ |
| 19 | CHANNEL PHASE POLYNOMIAL COEFFICIENT2 | 81 | IEEE754LSBDouble | 8 | n/a | The channel phase polynomial coefficient of degree 2 (expressed in $\text{rad}/(2\pi)/\text{s}^2$). This item has to be referred to the second boundary, as provided by item TIME TAG SECOND OF DAY. ⁶⁾ |
| 20 | CHANNEL PHASE POLYNOMIAL COEFFICIENT3 | 89 | IEEE754LSBDouble | 8 | n/a | The channel phase polynomial coefficient of degree 3 (expressed in $\text{rad}/(2\pi)/\text{s}^3$). This item has to be referred to the second boundary, as provided by item TIME TAG SECOND OF DAY. ⁶⁾ |
| 21 | END LABEL | 173 | SignedLSB4 | 4 | n/a | End label for data synchronization check. The value shall be equal to -99999. ⁷⁾ |

¹⁾ The value shall be equal to $2 \cdot (\text{SAMPLE RATE} \cdot \text{SAMPLE SIZE}) / 8 + \text{HEADER SIZE}$ in bytes, where $\text{HEADER SIZE} = 176$ bytes.

²⁾ $\text{SAMPLE RATE} \cdot 2 \cdot \text{SAMPLE SIZE}$ shall be a multiple of 32, to keep the sample word length to 32 bits.

³⁾ The downconversion value given here can either represent a physical ground station frequency difference or a logical downconversion.

⁴⁾ The downconversion from IF to the channel center frequency is represented as the sum of two parameters: a fixed value in IF_TO_CHANNEL_DOWNCONV and a variable value in CHANNEL POLYNOMIAL COEFFICIENT $_n$ where n is from 0 to 3.

⁵⁾ This parameter should give the total accumulated phase at the beginning of the frame except the additional channel phase polynomial contribution.

⁶⁾ To facilitate data processing the downconverter phase represented by the phase polynomial should be continuous in phase and phase rate from one second to the next.

⁷⁾ Entries between locations 97 and 172 are reserved for future use, and currently not used.

Table 13 gives the structure of the data block of L1 binary records provided in Delta-DOR RDEF Product File. It is similar to the data structure in the K5/VSSP and K5/VSSP32 formats in the sense that there are two nested groups, the outer group being the data block itself and the inner one being the 32-Bit Word Packing for the 8-Bit Sample case. However, within the inner group there are two fields, one giving the in-phase sample, the other one giving the quadrature-phase sample for the 8-Bit Sample case. In order to obtain actual data values, signed values need to be derived by applying two's complement to the unsigned 8-bit samples. If k is the signed value resulting from the two's complement operation, the actual data value v is then given by the transformation

$$v = 2k + 1. \quad (7)$$

Table 13: Structure of the data section in Level 1 binary records in Delta-DOR RDEF Product File with 8 bit of sample size

| Group no. | | Name | Group location (byte) | Repetitions | Group length (byte) | | Description |
|-----------|---|---|-------------------------|-------------------------------|-----------------------------|---------------|--|
| 1 | | Data Section | 177 | 0.5*SAMPLE RATE ¹⁾ | 2*SAMPLE RATE ¹⁾ | | Data Section. |
| | 1 | Sample 32-Bit Word Packing for 8-Bit Samples case | 1 | 2 | 4 | | Sample 32-Bit Word Packing for 8-Bit Samples case. |
| | | Field no. | Name | Location (byte) | Data type | Length (byte) | Description |
| | | 1 | In-phase Sample | 1 | UnsignedByte | 1 | In-phase sample for 8-Bit Sample case. |
| | | 2 | Quadrature-phase Sample | 2 | UnsignedByte | 1 | Quadrature-phase sample for 8-Bit Sample case. |

¹⁾ Number of repetitions and group length varies depending on sample rate and sample size. Sample rate is given in field no. 7 of the header section (see [Table 7](#)).

4.2.2 Level 2 – Calibrated Data

The RS calibrated data product consists of Doppler and signal amplitude measurements derived from Akatsuki radio occultations. They are reported as time series of the Doppler frequency and the signal level. Data at Level 2 and higher are only provided for radio occultations observing Venus. For each radio occultation, data is provided as a time-ordered ASCII table with 17 columns and a variable number of rows. [Table 14](#) provides a detailed description of each column reported in Level 2 ASCII tables.

Table 14: Fields of Level 2 ASCII tables.

| | Name | Data Type | Unit | Description |
|---|----------------------------|---------------------------|------|--|
| 1 | Sample Number | ASCII_NonNegative_Integer | n/a | The number of this row in the table, starting from 1 in the first row. |
| 2 | UTC Time | ASCII_Date_Time_YMD | n/a | The receiver date and time of this measurement in UTC. |
| 3 | Day-Of-Year with fractions | ASCII_Real | day | The day-of-year (and fraction) corresponding to "UTC Time" (field number 2) where 1.0000000000 is at YYYY-01-01T00:00:00 where YYYY is the current year in 4 digits. |
| 4 | Ephemeris Seconds | ASCII_Real | s | Seconds from 12h 1 January 2000 TDB (2000-01-01T12:00:00 TDB) corresponding to "UTC Time" (field number 2); includes leap seconds, if any. |

| | Name | Data Type | Unit | Description |
|----|--|---------------------|------|---|
| 5 | Distance | ASCII_Real | km | The impact parameter of the downlink geometric ray with respect to Venus for the photon received at the "UTC Time" (field number 2) in the absence of Venus atmosphere. |
| 6 | Transmit Frequency Ramp Reference Time | ASCII_Date_Time_YMD | n/a | The time t_0 at which the transmitted frequency would have been f_t using the coefficients f_0 ("Transmit Frequency - Constant Term" in field number 7) and df ("Transmit Frequency - Linear Term" in field number 8). At any time t within the interval when those coefficients are valid, the transmitted frequency f_t may be calculated from $f_t = f_0 + df * (t - t_0)$. If the transmit time is not known or is irrelevant, the value 1900-01-01T00:00:00.000 may appear. |
| 7 | Transmit Frequency - Constant Term | ASCII_Real | Hz | The initial frequency f_0 of the transmit frequency ramp (at t_0). See description of "Transmit Frequency Ramp Reference Time" (field number 6). |
| 8 | Transmit Frequency - Linear Term | ASCII_Real | Hz/s | The time derivative (df) of the transmitted frequency during the interval beginning at t_0 . See description of "Transmit Frequency Ramp Reference Time" (field number 6). |
| 9 | Observed X-Band Antenna Frequency | ASCII_Real | Hz | Frequency of the signal at the receiving antenna at "UTC Time (field number 2)". |
| 10 | Predicted X-Band Antenna Frequency | ASCII_Real | Hz | Expected frequency of the signal at the receiving antenna at "UTC Time" (field number 2) based on the Akatsuki reconstructed SPKs. The calculation includes geometrical effects (relative positions and motions of ground station and spacecraft, including the Earth rotation and light time adjustments). Correction for propagation through the Earth's neutral atmosphere is not made. |
| 11 | Correction of Earth Atmosphere Propagation | ASCII_Real | Hz | Frequency correction term for the propagation of the signal in the Earth atmosphere. |
| 12 | Residual Calibrated X-Band Frequency Shift | ASCII_Real | Hz | Value of "Observed X-Band Antenna Frequency" (field number 9) minus value of "Predicted X-Band Antenna Frequency" (field number 10). |
| 13 | Signal Level X-Band | ASCII_Real | none | Signal level in arbitrary linear unit with the effect of inaccurate antenna pointing corrected (relative unit). |
| 14 | Differential Doppler | ASCII_Real | Hz | Contribution of dispersive media to the received signal frequency calculated from two coherent bands. |
| 15 | Sigma Observed X-Band Antenna Frequency | ASCII_Real | Hz | A statistical measure of the error in determining "Observed X-Band Antenna Frequency" (field number 9). |

| | Name | Data Type | Unit | Description |
|----|---------------------------|------------|------|--|
| 16 | Signal Quality X-Band | ASCII_Real | none | Ratio of observed received signal strength to the statistical standard deviation of the measurement in dB. |
| 17 | Sigma Signal Level X-Band | ASCII_Real | none | A statistical measure of the error in determining "Signal Level X-Band" (field number 13). |

4.2.3 Level 3 – Derived Data

The L3 data product consists of refractivity, bending angle and, impact parameter profiles derived from Venus Climate Orbiter Akatsuki radio occultation data. The raw data were processed to level 2 and converted to bending angles and impact parameters. These results were then inverted to refractive index and refractivity via an Abel transform. Separate files are provided for ingress measurements and egress measurements. Data is provided as a time-ordered ASCII table with 19 columns and a variable number of rows. [Table 15](#) provides a detailed description of each column reported in Level 3 ASCII tables.

Table 15: Fields of Level 3 ASCII tables.

| | Name | Data Type | Unit | Description |
|---|---|---------------------------|----------|---|
| 1 | Sample Number | ASCII_NonNegative_Integer | n/a | The number of this row in the table, starting from 1 in the first row. |
| 2 | UTC Time | ASCII_Date_Time_YMD | n/a | The receiver date and time of this measurement in UTC. |
| 3 | Ephemeris Seconds | ASCII_Real | s | Seconds from 2000-01-01T12:00:00 TDB corresponding to "UTC Time" (field number 2); includes leap seconds, if any. |
| 4 | Residual Calibrated X-Band Frequency Shift | ASCII_Real | Hz | Observed sky frequency minus predicted frequency both taken from level 2 data product averaged for new sampling time. |
| 5 | Residual Calibrated X-Band Frequency Shift after Baseline Fit | ASCII_Real | Hz | The impact parameter of the downlink Value of "Residual Calibrated X-Band Frequency Shift" (field number 4) after subtraction of a polynomial to correct for non-atmospheric effects. |
| 6 | Reconstructed Transmit Frequency | ASCII_Real | Hz | Reconstructed transmitted frequency of the spacecraft. |
| 7 | Radius | ASCII_Real | km | Closest approach of the bended ray to the planet. The value gives the distance between the bended ray and the center of the planet. |
| 8 | Sigma Radius | ASCII_Real | km | One standard deviation uncertainty in "Radius" (field number 7). |
| 9 | Bending Angle | ASCII_Real | 1e-6 rad | Total bending angle measured as the angle between the ray asymptotes of the radio ray link. |

| | Name | Data Type | Unit | Description |
|----|------------------------|------------|----------|--|
| 10 | Sigma Bending Angle | ASCII_Real | 1e-6 rad | One standard deviation uncertainty in "Bending Angle" (field number 9). |
| 11 | Refractive Index | ASCII_Real | none | Refractive index of the atmosphere |
| 12 | Refractivity | ASCII_Real | none | Refractivity of the atmosphere. |
| 13 | Sigma Refractivity | ASCII_Real | none | One standard deviation uncertainty in "Refractivity" (field number 12). |
| 14 | Signal Level | ASCII_Real | none | Signal level in arbitrary linear unit with the effect of inaccurate antenna pointing corrected (relative unit). |
| 15 | Differential Doppler | ASCII_Real | Hz | Contribution of dispersive media to the received signal frequency calculated from two coherent bands. |
| 16 | Impact Parameter | ASCII_Real | km | Distance of the ray asymptotes to the planet. The value is defined as the distance between the ray asymptote and the center of planet. |
| 17 | Sigma Impact Parameter | ASCII_Real | km | A statistical measure of the error in determining "Signal Level X-Band" (field number 13). |
| 18 | Longitude | ASCII_Real | deg | East longitude of measurement in body fixed coordinates. |
| 19 | Latitude | ASCII_Real | deg | North latitude of measurement in body fixed coordinates. |

4.2.4 Level 4 - Derived Data

The L3 data product consists of Atmospheric density, pressure, and temperature profiles as a function of cytherocentric tangent radius including cytherolocation derived from Akatsuki radio occultation data. The atmospheric Doppler frequency time series observed at the ground station was converted to bending angle as a function of impact parameter. These results were then inverted to refractive index as a function of radius via an Abel transform. Number density was obtained from refractive index using a conversion formula appropriate to the known composition of the atmosphere (Sec. 3.1). Pressure and temperature profiles were derived by assuming hydrostatic balance and using the ideal gas law. Separate files are provided for ingress measurements and egress measurements. Data is provided as a time-ordered ASCII table with 24 columns and a variable number of rows. Because of the time-ordering of the data, ingress measurements have typically decreasing radii with time while egress measurements have typically increasing radii. [Table 16](#) provides a detailed description of each column reported in Level 4 ASCII tables.

Table 16: Fields of Level 4 ASCII tables.

| | Name | Data Type | Unit | Description |
|---|---------------|---------------------------|------|--|
| 1 | Sample Number | ASCII_NonNegative_Integer | n/a | The number of this row in the table, starting from 1 in the first row. |

| | Name | Data Type | Unit | Description |
|----|---|---------------------------|--------------------------------|--|
| 2 | UTC Time | ASCII_Date_Time_YMD | n/a | The receiver date and time of this measurement in UTC. |
| 3 | Ephemeris Seconds | ASCII_Real | s | Seconds from 2000-01-01T12:00:00 TDB corresponding to "UTC Time" (field number 2); includes leap seconds, if any. |
| 4 | Radius | ASCII_Real | km | Radius with respect to the center of the planet at measurement location. |
| 5 | Latitude | ASCII_Real | deg | North latitude at measurement location. |
| 6 | Longitude | ASCII_Real | deg | East longitude at measurement location. |
| 7 | Geopotential | ASCII_NonNegative_Integer | m ² /s ² | Geopotential at measurement location. |
| 8 | Geopotential Height | ASCII_Real | km | Geopotential height calculated from "Geopotential" (field number 7). |
| 9 | Pressure (Lower Temperature at Boundary) | ASCII_Real | Pa | Atmospheric pressure at "Radius" (field number 4) from the center of the planet calculated using the lower temperature of 140 K for the upper boundary condition. |
| 10 | Sigma Pressure (Lower Temperature at Boundary) | ASCII_Real | Pa | One standard deviation uncertainty in "Pressure (Lower Temperature at Boundary)" (field number 9). |
| 11 | Pressure (Medium Temperature at Boundary) | ASCII_Real | Pa | Atmospheric pressure at "Radius" (field number 4) from the center of the planet calculated using the medium temperature of 170 K for the upper boundary condition. |
| 12 | Sigma Pressure (Medium Temperature at Boundary) | ASCII_Real | Pa | One standard deviation uncertainty in "Pressure (Medium Temperature at Boundary)" (field number 11). |
| 13 | Pressure (Higher Temperature at Boundary) | ASCII_Real | Pa | Atmospheric pressure at "Radius" (field number 4) from the center of the planet calculated using the higher temperature of 200 K for the upper boundary condition. |
| 14 | Sigma Pressure (Higher Temperature at Boundary) | ASCII_Real | Pa | One standard deviation uncertainty in "Pressure (Higher Temperature at Boundary)" (field number 13). |
| 15 | Temperature (Lower Temperature at Boundary) | ASCII_Real | K | Atmospheric temperature at "Radius" (field number 4) calculated using the lower temperature of 140 K for the upper boundary condition. |
| 16 | Sigma Temperature (Lower Temperature at Boundary) | ASCII_Real | K | One standard deviation uncertainty in "Temperature (Lower Temperature at Boundary)" (field number 15). |
| 17 | Temperature (Medium Temperature at Boundary) | ASCII_Real | K | Atmospheric temperature at "Radius" (field number 4) calculated using the medium |

| | Name | Data Type | Unit | Description |
|----|--|------------|-----------------|---|
| | | | | temperature of 170 K for the upper boundary condition. |
| 18 | Sigma Temperature (Medium Temperature at Boundary) | ASCII_Real | K | One standard deviation uncertainty in "Temperature (Medium Temperature at Boundary)" (field number 17). |
| 19 | Temperature (Higher Temperature at Boundary) | ASCII_Real | K | Atmospheric temperature at "Radius" (field number 4) calculated using the higher temperature of 200 K for the upper boundary condition. |
| 20 | Sigma Temperature (Higher Temperature at Boundary) | ASCII_Real | K | One standard deviation uncertainty in "Temperature (Higher Temperature at Boundary)" (field number 19). |
| 21 | Number Density | ASCII_Real | m ⁻³ | Molecular number density of the atmosphere at "Radius" (field number 4). |
| 22 | Sigma Number Density | ASCII_Real | m ⁻³ | One standard deviation uncertainty in "Number Density" (field number 21). |
| 23 | Solar Zenith Angle | ASCII_Real | deg | Solar zenith angle at measurement location. |
| 24 | Local Solar Time | ASCII_Real | deg | Local solar time at measurement location. |

5 Applicable Software

5.1 Utility Programs

At the current time, the Venus Climate Orbiter Akatsuki project team has no plans to release any mission specific utility programs.

5.2 Applicable PDS Software Tools

Data products found in the Venus Climate Orbiter Akatsuki archive can be viewed with any PDS4 compatible software utility. A listing of these tools can be found at <https://pds.nasa.gov/tools/about/>.

5.3 Software Distribution and Update Procedures

As no Venus Climate Orbiter Akatsuki specific software will be released to the public, this section is not applicable.

6 Appendices

6.1 References

- CCSDS – The Consultative Committee for Space Data Systems, Recommended Standard for Delta-DOR Raw Data Exchange Format, CCSDS 506.1-B-1, 2013.
<https://public.ccsds.org/Pubs/506x1b1.pdf>
- Fjeldbo, G., Kliore, A. J., Eshleman, V.R., The neutral atmosphere of Venus as studied with the Mariner V radio occultation experiments, *Astron. J.*, **76**, 123–140, 1971.
- Ford, P. G., MGN V RDRS 5 GLOBAL DATA RECORD TOPOGRAPHIC V1.0, MGN-V-RDRS-5-GDR-TOPOGRAPHIC-V1.0, NASA Planetary Data System,
<https://doi.org/10.17189/1522522>, 1992
- Häusler, B., Pätzold, M., Tyler, G. L., Simpson, R. A., Bird, M. K., Dehant, V., Barriot, J.-P., Eidel, W., Mattei, R., Remus, S., Selle, J., Tellmann, S., Imamura, T., Radio science investigations by VeRa onboard the Venus Express spacecraft, *Planet. Space Sci.*, **54**, 1315–1335, 2006.
- Kondo, T., K5/VSSP and K5/VSSP32 Data Format, TDC Tec. Rep., National Institute of Information and Communications Technology, 2010,
https://www2.nict.go.jp/sts/stmg/K5/VSSP/vssp_format-e.100820.pdf
- Imamura, T., et al., RS: Radio Science investigation of the Venus atmosphere and ionosphere with Venus orbiter, Akatsuki, *Earth Planets Space*, **63**, 493–501,
<https://doi.org/10.5047/eps.2011.03.009>, 2011.
- Imamura, T., et al., Initial performance of the radio occultation experiment in the Venus orbiter mission Akatsuki, *Earth Planets Space*, **69**, 137, <https://doi.org/10.1186/s40623-017-0722-3>, 2017.
- Ogohara, K., et al., Overview of Akatsuki data products: definition of data levels, method and accuracy of geometric correction, *Earth, Planets and Space*, **69**, 167,
<https://doi.org/10.1186/s40623-017-0749-5>, 2017.
- Seiff, A., et al., Models of the structure of the middle atmosphere of Venus from the surface to 100 kilometers altitude. *Adv. Space Res.*, **5**, 1–305, 1985.
- Tellmann, S., Pätzold, M., Häusler, B., Bird, M. K., Tyler, G. L., Structure of the Venus neutral atmosphere as observed by the Radio Science experiment VeRa on Venus Express. *J. Geophys. Res.*, **114**, E00B36, <https://doi.org/10.1029/2008JE003204>, 2009.
- Toda T., Hayashiyama T., Kamata Y., Ishii N., Nakamura M., Flight model development of PLANET-C telecommunication subsystem. In: The 27th International Symposium on Space Technology and Science, Transactions of Japan Society for Aeronautical and Space Sciences, Space Technology Japan 8, No. 27, 17-22, 2010.

6.2 Definitions of Data Processing Levels

PDS4 Data Processing Levels (From PDS Policy on Data Processing Levels (2013-03-11):

Telemetry: An encoded byte stream used to transfer data from one or more instruments to temporary storage where the raw instrument data will be extracted.

Raw: Original data from an instrument. If compression, reformatting, packetization, or other translation has been applied to facilitate data transmission or storage, those processes will be reversed so that the archived data are in a PDS approved archive format.

Partially Processed: Data that have been processed beyond the raw stage but which have not yet reached calibrated status.

Calibrated: Data converted to physical units, which makes values independent of the instrument.

Derived: Results that have been distilled from one or more calibrated data products (for example, maps, gravity or magnetic fields, or ring particle size distributions). Supplementary data, such as calibration tables or tables of viewing geometry, used to interpret observational data should also be classified as ‘derived’ data if not easily matched to one of the other three categories.